8

Imaging Manifestations and Techniques in Diabetes Insipidus

Nirmal Phulwani, Tulika Pandey,
Jyoti Khatri, Raghu H. Ramakrishnaiah,
Tarun Pandey and Chetan C. Shah
University of Arkansas for Medical Sciences, Little Rock, Arkansas
United States of America

1. Introduction

Diabetes insipidus (DI) is a clinical condition characterized by excretion of large volume of low specific gravity urine (1). Diabetes insipidus can be central in which there is deficient production of arginine vasopressin (AVP) also known as anti-diuretric hormone (ADH) or nephrogenic in which there is end organ resistance to ADH action (1).

2. Classification

Etiological classification of diabetes insipidus is as follows.

1. Central Diabetes Insipidus (CDI)
   - A. Idiopathic
   - B. Familial
   - C. Structural Causes
     - i. Congenital: Septo-optic dysplasia
       Tuber cinereum Hamartoma
     - ii. Traumatic: Iatrogenic, head trauma
     - iii. Inflammatory: Tuberculous Meningitis
       Sarcoidosis
       Wegener's granulomatosis
       Lymphocytic Hypophysitis
     - iv. Neoplastic:
       - a. Pediatric:
         Hypothalamic glioma
         Craniopharyngioma
         Intracranial Germ Cell Tumors
         Teratoma
         Langerhans Histiocytosis
       - b. Adult: Metastasis
2. Psychogenic: Compulsive intake of large amounts of fluid leading to inhibition of normal vasopressin (2).

3. Nephrogenic Diabetes Insipidus (NDI)
   A. Primary
   B. Secondary: Polycystic kidney disease, drug toxicity such as Lithium toxicity, analgesic nephropathy, reflux nephropathy, amyloidosis, acute tubular nephropathy (1)

3. Etiopathogenesis

Central diabetes insipidus is characterized by decreased secretion of ADH that results in polyuria and polydipsia by diminishing the patient's ability to concentrate urine. Diminished or absent ADH can be the result of a defect in one or more sites involving the hypothalamic osmoreceptors, supraoptic or paraventricular nuclei, or the supraopticohypophyseal tract. In contrast, lesions of the posterior pituitary rarely cause permanent diabetes insipidus, because the ADH is produced in the hypothalamus and still can be secreted into the circulation (1, 3).
Psychogenic diabetes insipidus is caused by compulsive intake of large amounts of fluid leading to inhibition of normal vasopressin (2).
Nephrogenic diabetes insipidus is characterized by a decrease in the ability to concentrate the urine due to resistance to ADH action in the kidney. NDI can be observed chronic renal insufficiency, Lithium toxicity, Hypocalcaemia and tubular interstitial disease (1, 4, 5).

4. Relevant anatomy

Sella turcica is a saddle shaped fossa located in the sphenoid bone. It is bounded by the prechiasmal sulcus, tuberculum sella and by the anterior clinoid processes. Sphenoid sinus lies below and anterior to it. The bony margins of sella are best seen with computed tomography (CT scan). The fatty bone marrow of the bones of the sella creates hyperintense T1 signal on magenetic resonance imaging (MRI). Suprasellar cistern is a CSF space located just above the sella and contains vessels forming the circle of Willis. Optic chiasm is located within the center of suprasellar cistern. On lateral aspect, pair of cavernous sinuses exist which contain internal carotid artery along with oculomotor, trochlear and abducent nerves in addition to the first and second divisions of trigeminal nerve (6, 7).
The pituitary gland occupies the sella turcica and consists of two parts called as anterior (adenohypophysis) and posterior (neurohypophysis) pituitary. These lobes are developmentally and functionally different. Anterior pituitary is formed from the evagination of oral ectodermal tissue called Rathke's pouch, which is derived from the nasopharyngeal tissue during the embryonic period. Posterior pituitary is derived from diencephalic neuroectoderm and is connected to the hypothalamus via pituitary stalk. Antidiuretic hormone and vasopressin are formed in the hypothalamus and travel to the posterior pituitary and are stored there. The pars intermedia is located between the anterior and posterior pituitary and is regarded as vestigial (6-8).
Anterior pituitary constitutes the 75% of entire pituitary volume and occupies the anterior portion of sella turcica. Posterior pituitary occupies the central portion of sella turcica and is surrounded on both sides by two wings of anterior lobe. MRI easily distinguishes both anterior and posterior pituitary lobe. Posterior pituitary often manifests as markedly hyperintense on T1 weighted images and moderately hyperintense on T2 weighted imaging due to the presence of arginine-vasopressin in neurohypophysis. Entire pituitary gland shows contrast enhancement (figure 1) on both CT and MRI (6-8).

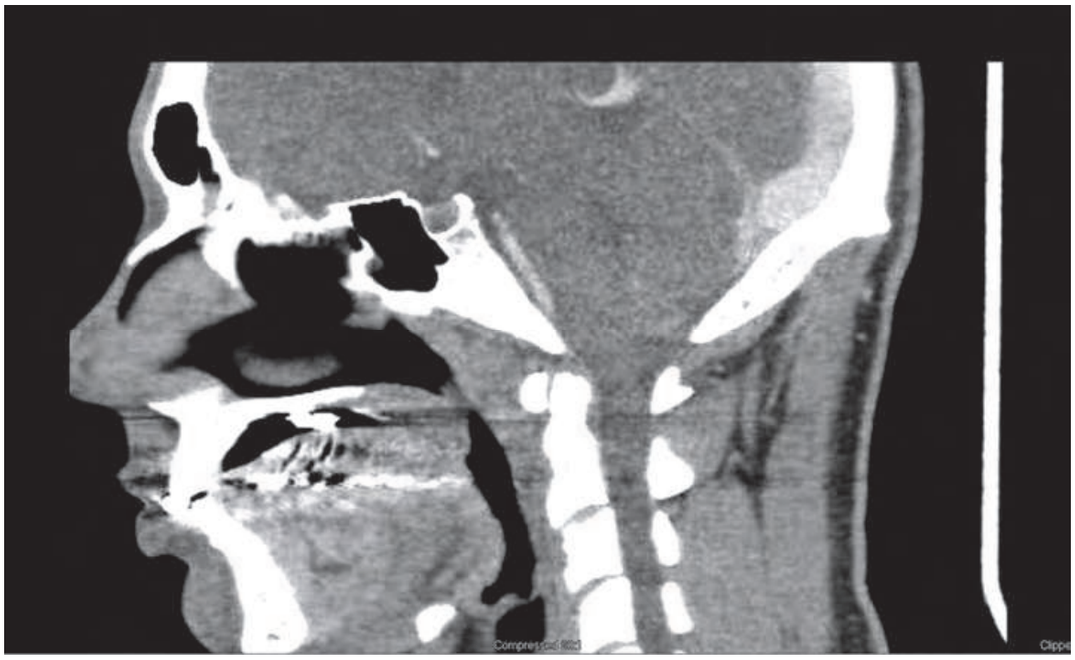

(a)

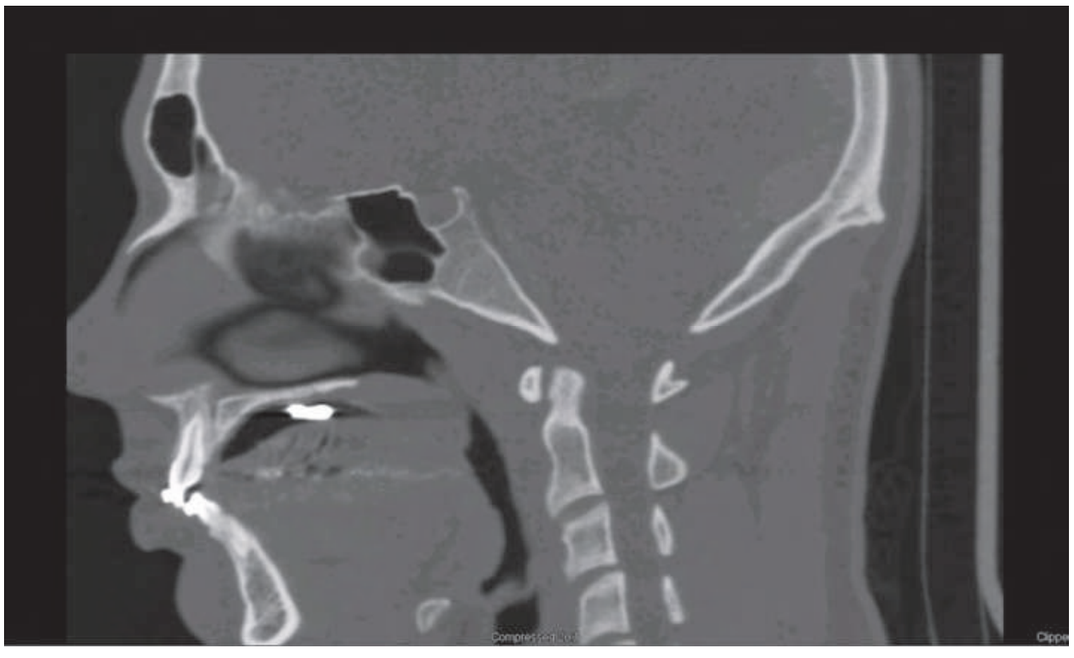

(b)

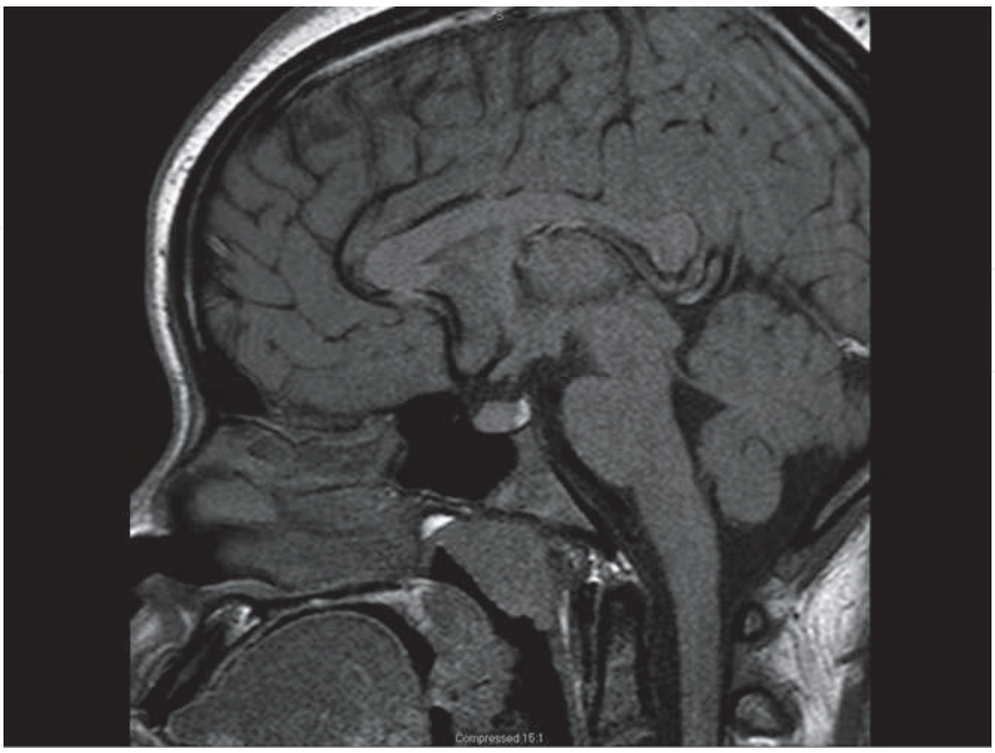

(c)

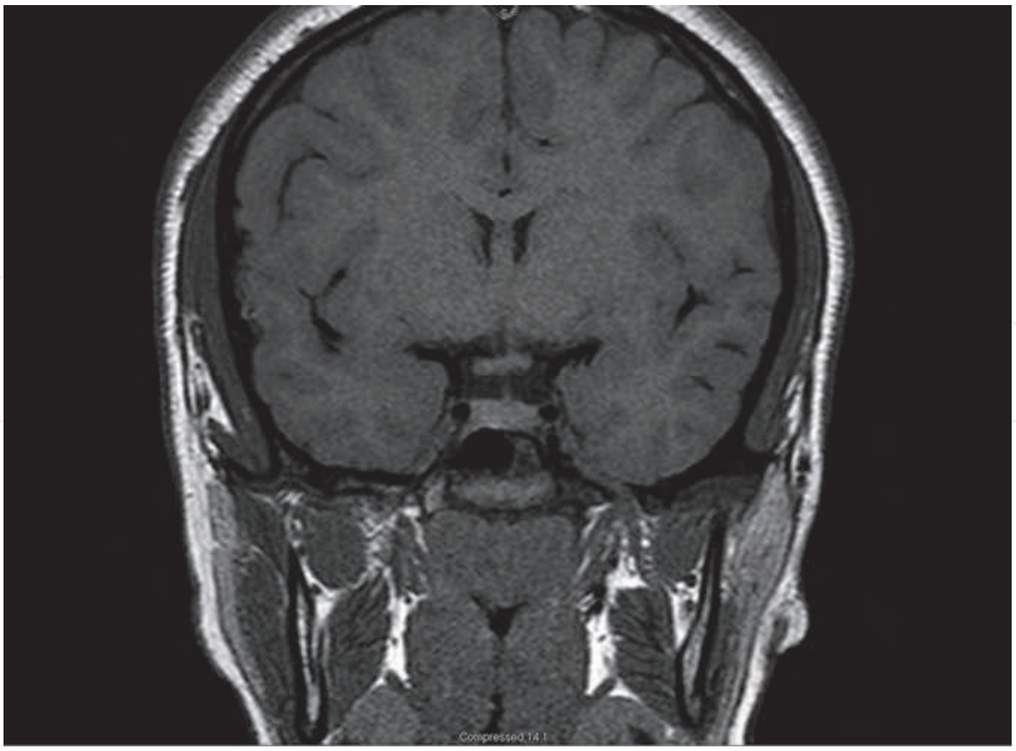

(d)

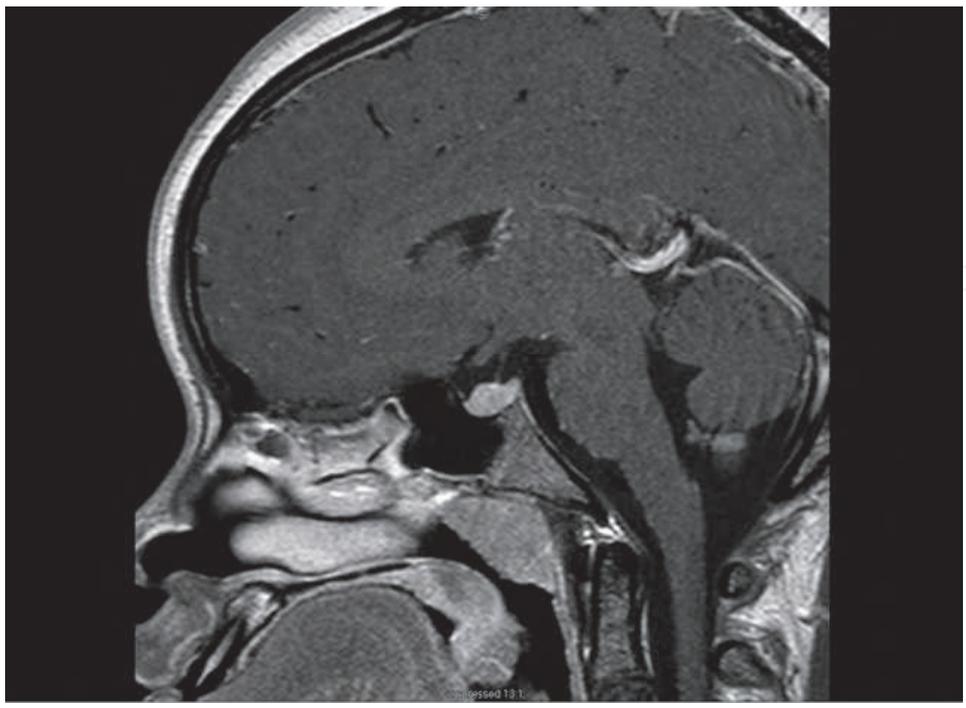

(e)

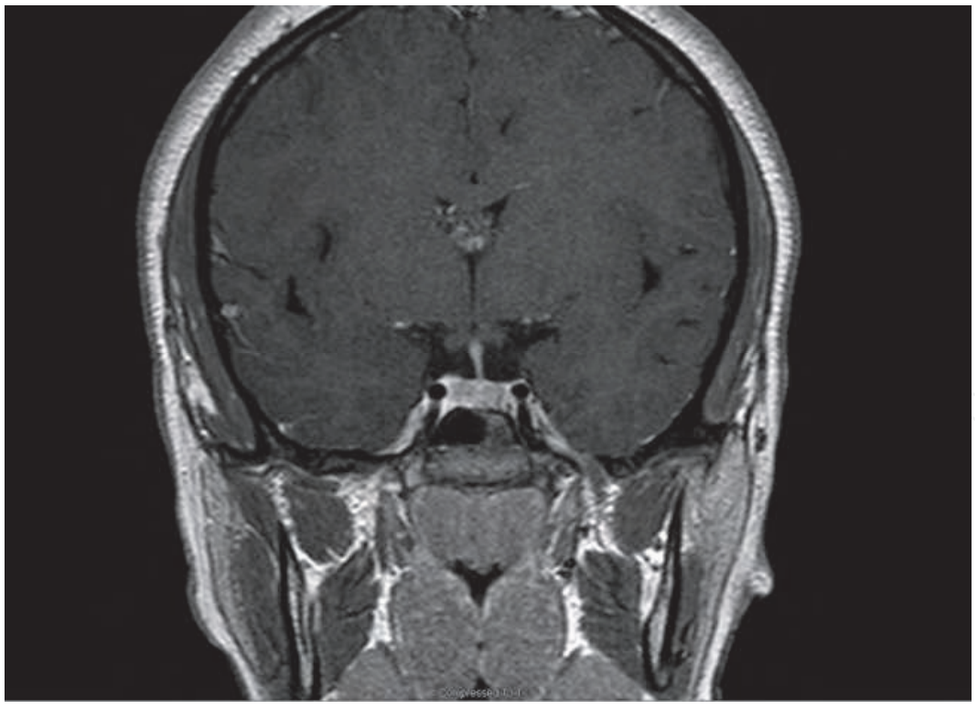

(f)

Normal precontrast sagittal(1c), coronal (1d), post contrast sagittal (1e) and coronal (1f) MRI of pituitary stalk and pituitary gland

Fig. 1. Normal CT sagittal post contrast soft tissue window (1a) and bone algorithm (1b)

The hypothalamus is the ventral part of diencephalon and extends from lamina terminalis to a vertical plane posterior to the mamillary bodies and from hypothalamic sulcus to the pial surface of the floor of the third ventricle (5-6).
Posterior lobe of the pituitary has rich and direct blood supply which explains extensive immediate contrast enhancement of posterior lobe. Anterior pituitary is supplied by the portal pituitary system which explains delay in contrast accumulation in anterior pituitary lobe compared to the posterior pituitary lobe. Similarly, due to relatively deficient vascular supply of anterior lobe, it is more vulnerable to ischemic insults such as Sheehan's syndrome and pituitary apoplexy (6).
Dimensions and shape of pituitary are variable during different physiological states. At birth, pituitary is usually globular in shape and reveals hyperintensity on T1 weighted images in both anterior and posterior lobe. At about 6 weeks of postnatal life, anterior lobe loses hyperintensity and become isointense to that of cerebral white matter. On the other hand, posterior pituitary retains its hyperintensity which serves as an important landmark throughout the life. Pituitary is usually larger in size in female and further increases during pregnancy. Also at adolescent, pituitary size increases physiologically. Despite variations in size, shape and height, pituitary gland should fill the whole sella turcica with variations in height (6-8).

5. Role of imaging

MR imaging is the modality of choice for evaluating central diabetes insipidus due to its multiplanar imaging capability, better tissue contrast resolution and capability to selectively suppress individual tissue signal like fat. CT scan is better than MRI for detecting calcifications, bone destruction and osteolytic lesions (6-8).

5.1 MR imaging protocol

Coronal T1, coronal T2, small field of view sagittal T1 weighted images of the sella with and without fat saturation are obtained., After injection of the intravenous contrast, fat suppressed sagittal and coronal T1 weighted images of the sella are also obtained. MRI of the brain with and without contrast is also performed for a comprehensive evaluation of the pituitary, sellar and parasellar region (6).
Nephrogenic diabetes insipidus is characterized by a decrease in the ability to concentrate urine due to resistance to ADH action in the kidney. Diagnosis of NDI is often clinical and laboratory based and imaging has marginal benefit in this group of DI (1, 4, 5).

6. Central Diabetes Insipidus (CDI)

6.1 Idiopathic Central Diabetes Insipidus

It is the most common type of diabetes insipidus (DI) and is seen in 30-50 % of patients diagnosed with CDI. It has been suggested that idiopathic CDI is an autoimmune disease characterized by the lymphocytic infiltration of posterior pituitary and pituitary stalk. The role of autoimmunity is evident from the association of this disease with other autoimmune conditions and presence of cytoplasmic antibodies against the vasopressin. On MRI, posterior pituitary and pituitary stalk often appear thickened and enlarged, particularly during the early stage. Such presentation is more common in young female patients. However, thickening of pituitary is a non specific finding since patient having such

presentation on the MRI, may develop germinoma or histiocytosis. Particularly, progressive thickening of pituitary stalk in pediatric patients on serial MRIs is often due to germinoma. In addition, other endocrine abnormalities are also seen in such patients including suppressed release of growth hormone (GH), thyroid stimulating hormone (TSH) and adrenocorticotropic hormone (ACTH) (3).

6.2 Familial Central Diabetes Insipidus

Familial CDI or familial neurohypophyseal diabetes insipidus (FNDI) is often an autosomal dominant disease which is caused by mutations in the arginine-vasopressin gene (AVP). This mutation leads to accumulation of misfolded arginine-vasopressin fibrillar aggregates within the endoplasmic reticulum and causes death of the magnocellular neurons of SOP and PVN nuclei of hypothalamus. This phenomenon is called toxic gain of function and is also seen in other neurodegerative conditions such as Huntington disease and Parkinson disease. However, it is unclear how these aggregates cause death of magnocellular neurons. Children born with autosomal dominant disease often develop symptoms several months or years following the birth (9).

6.3 Structural causes

6.3.1 Congenital

Septo-optic Dysplasia:

Septo-optic Dysplasia (figure 2) is a disease spectrum with variable combination of the following components:

- Optic nerve hypoplasia
- Pituitary abnormality such as ectopic posterior pituitary
- Absent septum pellucidum

Septo-optic dysplasia is associated with abnormalities of cortical development and hypothalamic-pituitary dysfunction. Suppression of hypothalamic-pituitary axis leads to growth retardation secondary to suppressed release of growth hormone and TSH from the anterior pituitary. In addition, such involvement also affect serum level of ADH since ADH is released from the hypothalamus and stored in posterior pituitary before release into the circulation causing CDI. In addition, these children exhibit variable combinations of cleft palate, syndactyly, ear deformities, hypertelorism, optic atrophy, micropenis, and anosmia (10).

Affected children have mutations in the HESX1 gene, which is involved in early development of the ventral prosencephalon. Pituitary dysfunction leads to diabetes insipidus, GH deficiency and short stature, and, occasionally, TSH deficiency (11).

Posterior pituitary stores hormones released from the hypothalamic neurons which reach posterior pituitary via descending axons. These axons are covered by the ascending ectodermal cells of the Rathke's pouch as they migrate towards the posterior pituitary during development. The development of posterior pituitary is complete by the end of first trimester. Abnormality of the migration can lead to ectopic posterior pituitary gland located either near the median eminence or along the pituitary stalk (12).

Tuber Cinereum Hamartoma

Tuber Cinerium Hamartoma is a congenital disorder of defective neuronal migration characterized by gray matter heterotopias, formation of which typically begins during the

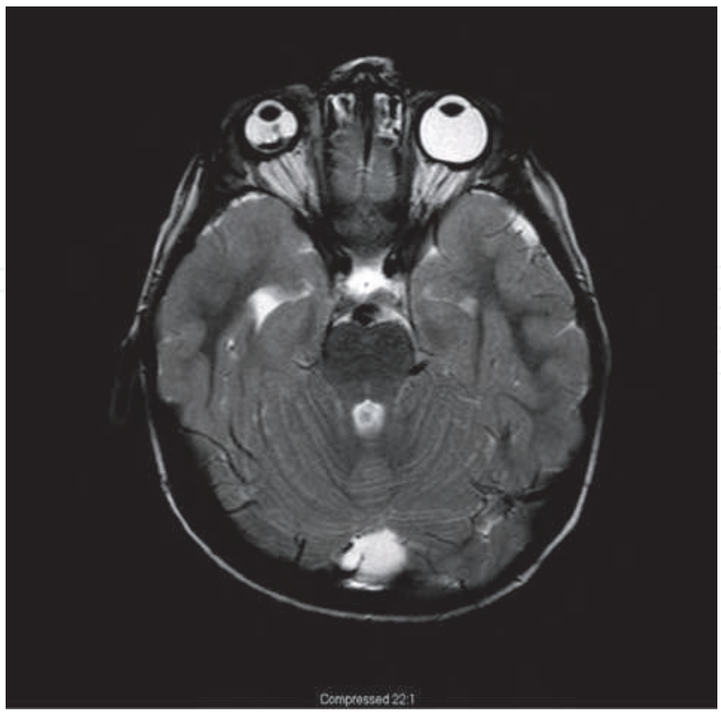

(a)

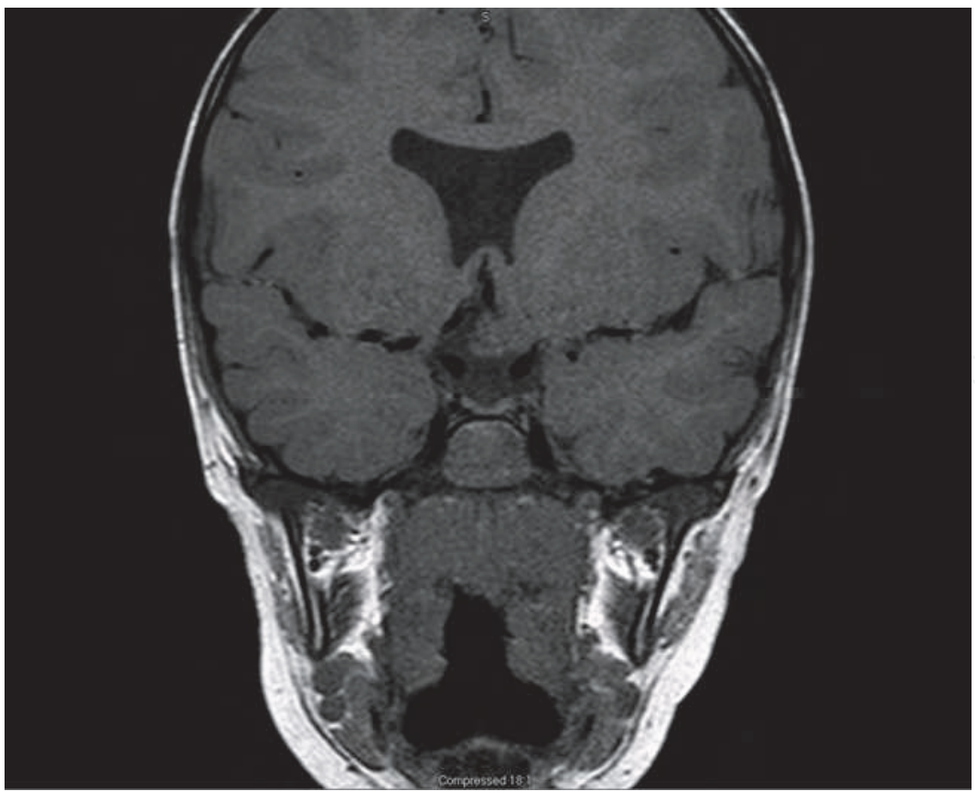

(b)

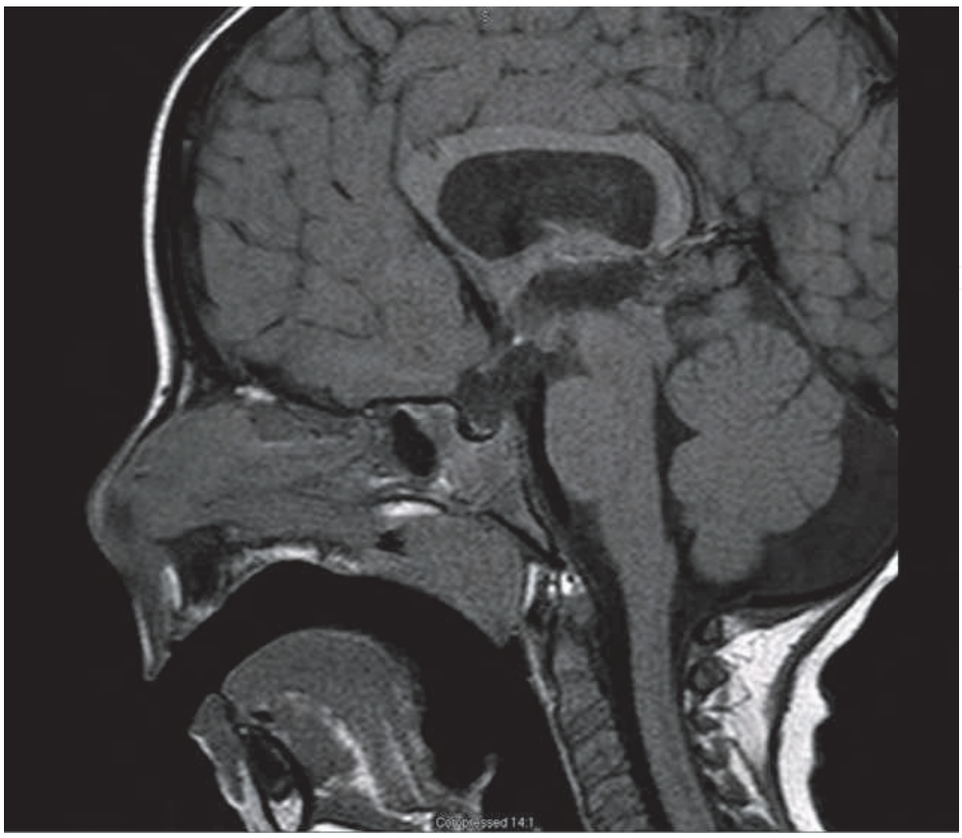

(c)

Fig. 2. MRI of Septo-Optic Dysplasia: Axial T2 (2a) shows bilateral optic nerve hypoplasia, right retinal detachment and right microophthalmia from retinopathy of prematurity. Coronal T1 (2b) shows absent septum pellucidum. Sagittal T1(2C) shows ectopic posterior pituitary bright spot.

days 33-41 of gestational life. It is approximately 1-3 cm in size, nonneoplastic and disorganized collection of hypothalamic neurons, glia and fiber bundles. It is typically located on the floor of third ventricle within the tuber cinereum of the hypothalamus. Recent literature suggested that tuber cinereum hamartoma accounts for about 33% of all cases of true precocious puberty and is seen more commonly in boys than girls. The precocious puberty seen in these patients develops about 2 years earlier than in idiopathic precocious puberty and patients are often less than 3 years of age (13-14).

The induction of precocious puberty is due to pulsatile release of GnRH from the hamartoma which leads to premature activation of hypothalamic-pituitary-gonadal axis. Occasionally patients present with acromegaly secondary to excessive growth hormone release from the Hamartoma. In addition to hormonal disturbances, patient often present with gelastic epilepsy (spasmodic or hysterical laughter) with interval irritability and depressed mood. In addition, several other malformations are also noted in association with tuber cinereum Hamartoma such as polydactyly, microgyria, hemispheric heterotopias, corpus callosum agenesis, mental retardation and behavioral problems. Occasionally, tuber cinereum hemartomas can be a part of Pallister-Hall syndrome which is caused because of a frameshift mutation of chromosome 7p13 and is characterized by multiple malformations,

such as polydactyly and imperforate anus. However, neurologic symptoms are less severe in patients with Pallister-Hall syndrome (13-14).

With smaller (3-15 mm) pedunculated mass, patient is often asymptomatic or may only have central precocious puberty. However, with large (10-38 mm) and sessile lesions, patient often display multiple symptoms including seizures. Radiography in patients with tuber cinereum hamartoma and precocious puberty show advanced bone age, evidence of intracranial calcification, increased intracranial pressure and enlarged sella turcica. In addition, ultrasonography shows enlargement of ovaries accompanied by several small cysts/follicles, prominence/enlargement of uterus and well defined central endometrial lining. CT has limited role due to decreased sensitivity at the level of sella turcica and shows isodense mass compared to the gray matter without any evidence of calcification and contrast enhancement. Therefore, MRI is the main modality for identifying hypothalamic hamartoma (figure 3) which shows isodense lesion to gray matter on T1 weighted images which do not enhance with contrast along with preservation of pituitary bright spot. On T2 weighted images Hamartoma is either isointense or slightly hyperintense compared to gray matter. Particularly, lack of enhancement helps to differentiate hypothalamic Hamartoma from germ cell tumor, Langerhans cell histiocytosis and hypothalamic glioma which are also seen in the same location and show at least partial uptake of contrast (13-14).

Recently, it has been reported that MR spectroscopy can also play an important role in diagnosis of tuber cinereum hamartoma with more information regarding the functional status of this mass. Since the mass is slow growing and rarely cause mass effect, initial treatment is symptomatic management and includes hormone suppressive therapy with leutenizing hormone antagonist such as leuprolide or continuous administration of GnRH analogs which effectively suppresses premature precocious puberty and seizures. Surgery is reserved for those patients having intractable seizures or rapid growth of mass with no benefit seen with hormone suppressive therapy (13-14).

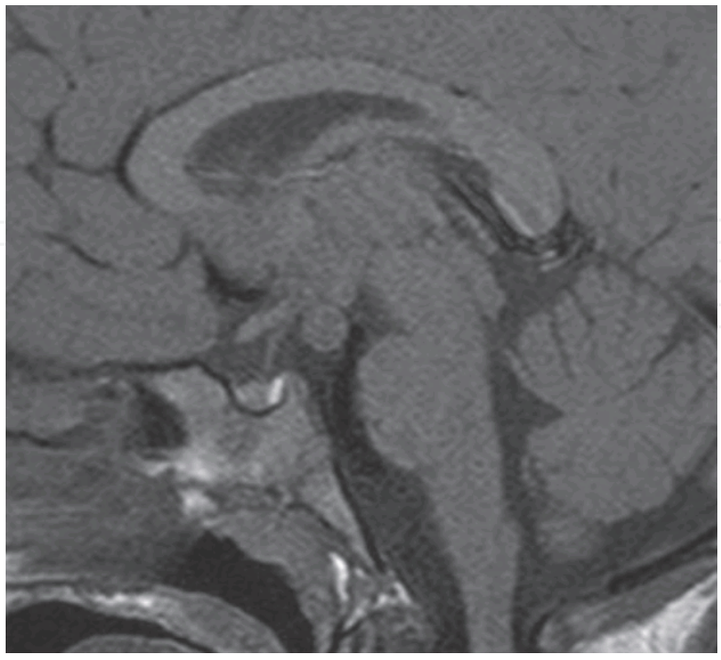

(a)

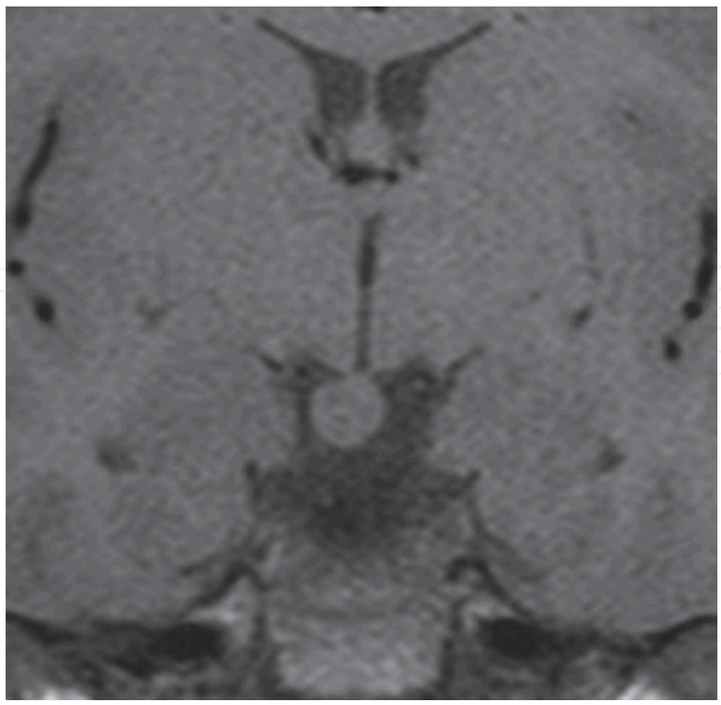

(b)

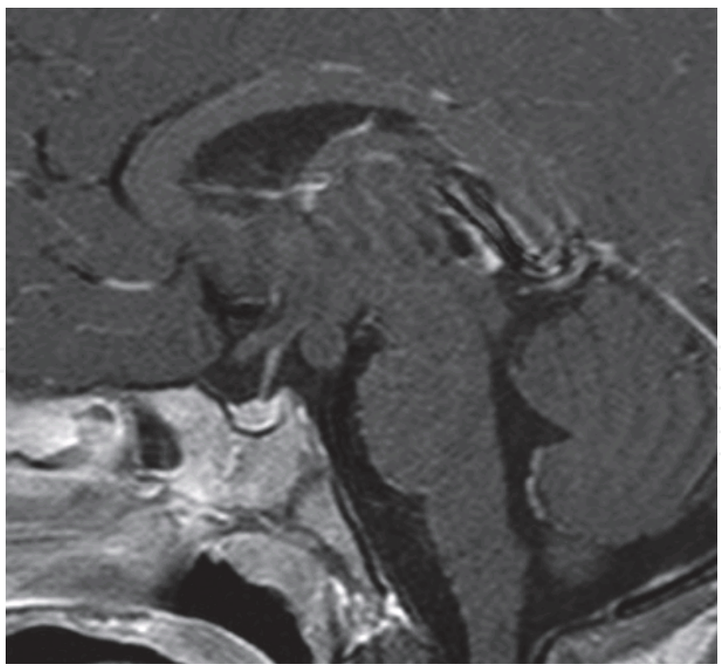

(c)

Fig. 3. Hypothalamic Hamartoma. Precontrast coronal (3a) and sagittal (3b) images show isointense lesion in the region of hypothalamus. Post contrast image (3c) show lack of enhancement of the lesion.

6.3.2 Traumatic

Iatrogenic injury from neurosurgical procedures especially after trans-sphenoidal surgery can lead to the CDI because of iatrogenic damage to the hypothalamus and posterior pituitary. For example, transsphenoidal removal of small tumors limited to sella has resulted in development of CDI. Whereas, removal of large tumors has been shown to precipitate CDI in as high as 60-80% of total patients. The incidence rate declines significantly in patients who have undergone minimally invasive endoscopic pituitary surgery (2.7% permanent and 13.6% transient). The likelihood of developing permanent CDI is higher if plasma sodium level reaches level higher than 145 mmol/L within the first five days postoperatively.

Occasionally, neurosurgery or head trauma causes severe damage to the hypothalamus and pituitary stalk. In such scenarios, often triphasic response is seen. In the beginning, polyuric phase is present which lasts up to 4-5 days and is due to inhibition of ADH release from the hypothalamus. This is followed by antidiuretic phase between days 6-11 that is characterized by the slow release of ADH from the posterior pituitary and leads to hyponatremia secondary to antidiuretic effects of ADH. Once the ADH store in posterior pituitary is depleted, patient develops permanent CDI. However, it is important to note that very often the damage to hypothalamic-pituitary axis is mild to moderate and does not cause permanent CDI. 3.4% of patients had transient polyuria and then transient hyponatremia. It is very important to realize that polyuria seen following a major surgery including neurosurgery is not always due to CDI and may result from excess IV fluids given during the surgery, and also from osmotic dieresis induced from administration of mannitol and glucocorticoid for minimizing the cerebral edema. These conditions can be differentiated from CDI by measuring urine osmolality and the response to water restriction and the administration of ADH. Usually, urine osmolality is less than plasma osmolality and less than 300 mOsm/kg and plasma AVP concentration is low in spite of high plasma osmolality in the CDI Rarely, patient develops combination of CDI and cerebral salt wasting following neurosurgery (15).

6.3.3 Inflammatory

Tuberculous meningitis

Tuberculous meningitis is aseptic meningitis which is often caused because of the spread of infection from the pulmonary focus via hematogeneous route but can also occur because of contiguous spread from adjacent focus of infection. The most common endocrinal disturbance noted is hyperprolactinemia followed by cortisol deficiency and central hypothyroidism. In addition, isolated cases of SIADH and CDI have also been reported.

Intracranial tuberculosis presents as sellar or suprasellar tuberculoma along with calcification, obstructive hydrocephalus, vasculitis or apoplexy. Characteristic MRI changes include sellar tuberculoma, osteomyelitis of adjacent bones, caseous necrosis, dural enhancement and exudates in and around the pituitary gland in addition to thickened pituitary stalk. Post contrast studies show nodularity or thickening of the stalk and infundibulum. The pituitary tuberculomas are heterogeneously isointense on T1 weighted imaging and hyperintense on T2 weighted imaging with intense enhancement with contrast. Occasionally, T1 weighted images show hyperintensity attributed to the high protein content and the non-enhancing areas are likely due to caseous necrosis (16).

Sarcoidosis

Sarcoidosis is a chronic noncaseating granulomatous disease characterized by abnormal collection of chronic inflammatory cells including lymphocytes, macrophages and multinucleated giant cells at various locations including lungs, lymph node, skin and neural tissue. It is more common in African American female. Disease course is often insidious and patient may remain asymptomatic. Occasional spontaneous remissions and improvements have been reported but relapse rate of more than 50% is also seen. About 10% patients develop serious morbidity due to pulmonary scarring and respiratory failure. However, other nonspecific symptoms include fatigue, difficulty to sleep, lack of energy and motivation, joint swelling and pain, blurry vision, skin rash, shortness of breath. Skin lesions include rash, erythema nodosum (swelling in front of anterior tibia or shin) and lupus pernio. There are some variants of sarcoidosis. For example, triad of erythema nodosum, bilateral hilar lymphadenopathy and arthalgia is called Lofgren syndrome that has good prognosis compared to other variants. Involvement of CNS is referred as neurosarcoidosis and is noted in 5% of patients diagnosed with sarcoidosis. In addition, about 33% of patients diagnosed with neurosarcoidosis develop some degree of CDI. In addition, occasional hypothalamic disturbances and defects in anterior pituitary hormonal release are also noted in such patients. Neurosarcoidosis affects leptomeninges, vascular structures, cranial nerves, hypothalamus, infundibular stalk and pituitary gland. DI is suggested to be due to the either vasculitis or direct granulomatous effect.

As with other inflammatory condition involving pituitary stalk, MRI shows uniformly thickened pituitary stalk but occasional involvement of adjacent hypothalamus and pituitary is seen. Similar to other granulomatous disease, strong contrast enhancement is also seen. Interestingly, such features on MRI are seen only in patients who have CDI for less than 2 years and are lost upon follow up suggesting that neurosarcoidosis induced DI is self limiting (17-18).

Wegener's granulomatosis

Wegener s granulomatosis (WG) is a systemic, necrotizing, granulomatous vasculitis of small and medium sized vessels that was first described in detail by Friedrich Wegener in 1939. It is a chronic disease of unknown etiology and is closely associated with elevated serum levels of anti-neutrophil cytoplasmic antibody (ANCA). Once diagnosis is established, WG require lifelong immunosuppresion because of propensity to cause irreversible end organ damage. It affects multiple organ systems, such as upper and lower airway involvement (sinusitis, epistaxis, dyspnea and cough), kidney (impaired kidney functioning, rapidly progressive glomerulonephritis and chronic kidney failure) and other organs. In about one third of patients, CNS is involved and patient exhibit features of peripheral neuropathy, mononeuritis multiplex, cranial nerve palsies, stroke, cerebral vasculitis and rarely CDI. Involvement of posterior pituitary in WG is very rare with only less than 50 cases described in literature so far since 1953. Due to rare association between WG and CDI, it is often missed during the early course of disease. Therefore, it is very important for physicians to suspect WG in any patient presenting with nasal congestion, epistaxis, dyspnea, polydipsia and polyuria. Definitive diagnosis is established by tissue biopsy that often shows leukocytoclastic vasculitis with granulomatous inflammation.

On MRI, WG-induced CDI appear as diffusely enlarged pituitary and infundibular stalk compared to optic chiasm and occasionally intrasellar mass is seen. In addition in some patients, cystic changes have been reported in pituitary and infundibulum but no contrast

enhancement is seen. Loss of posterior pituitary bright spot is seen on T1 weighted images (likely due to significant decrease in arginine-vasopressin content in posterior pituitary) and no contrast enhancement is noted. Occasionally, MRI failed to show any changes in pituitary in patients with proven clinical CDI and WG. In such patients, it has been suggested that CDI is caused because of small vessel vasculitis and therefore remain undetected. Treatment is often directed at immune suppression (19-20).

Lymphocytic infundibuloneurohypophysitis and lymphocytic adenohypophysitis

Lymphocytic Infundibuloneurohypophysitis and Lymphocytic Adenohypophysitis were initially identified as one of the most important causes of idiopathic DI. Lymphocytic Adenohypophysitis is a rare autoimmune disease which is seen more commonly in younger female of menstrual age and is acute in onset. Patients often have other autoimmune disease as well and are positive for autoantibodies against arginine-vasopressin secreting cells. It is not yet clear whether these antibodies are cytotoxic and cause DI via damaging the neural tissue. However, their presence indicates the high likelihood of development of overt DI in such patients. Such patients have long history of subclinical disease followed by clinically obvious DI.

MRI in lymphocytic adenohypophysitis typically shows pituitary infundibulum thickening and neurohypophysis enlargement in such patients. During the early subclinical phase, posterior lobe of pituitary is often hyperintense on MRI but become normal again indicating the self-limiting nature of this disease. Upon biopsy, inflammatory infiltrate consisting of T lymphocytes and plasma cells is identified in the affected tissues with occasional presence of macrophages, neutrophils and eosinophils in the anterior pituitary. Interestingly, treatment with DDAVP leads to recovery of posterior pituitary function along with disappearance of autoantibodies.

Lymphocytic Infundibuloneurohypophysitis presents with the combination of CDI and vision disturbances and might have serum positivity for autoantibodies against arginine-vasopressin secreting cells. Lymphoplasmacytic infiltrate is seen in hypothalamus, pituitary, infundibulum, optic nerve, tract and chiasm. MRI imaging in these patients show normal pituitary with focal nodular thickening of the infundibulum, stalk thickening, and absence of hyperintense signal of neurohypophysis. Occasionally, anterior pituitary is also affected. Overall, it is also a self-limiting disorder and no treatment is needed except hormone replacement for short duration of time. In addition, glucocorticoid therapy is also given to decrease the intracranial pressure (21-22).

6.3.4 Neoplastic

6.3.4.1 Pediatric neoplastic causes

Hypothalamic glioma

Hypothalamic gliomas are low-grade tumors arising from glial cells and are classified as World Health Organization grade I tumors. Despite low grade, these tumors are associated with higher morbidity and mortality. Very often these tumors are located in optic chiasmatic/hypothalamic region but are also seen in the posterior fossa, temporal lobe and spinal cord. Hypothalamic gliomas are commonly seen in childhood and adolescent age group. However, hypothalamic gliomas are occasionally seen in adults and are more aggressive than their pediatric counterparts. Male and female are equally affected.

About one third of the hypothalamic gliomas are associated with neurofibromatosis 1, which is an autosomal dominant disease resulting from mutation on chromosome 17. Patients who have associated NF1 have been reported to have better prognosis than those without NF1 and are characterized by smaller, often non-cystic lesions with more frequent involvement of the orbital portion of optic nerve. On the other hand, gliomas without associated NF1 are larger, cystic and frequently affect hypothalamus and optic chiasm. In severe cases, calcification is noted within the stroma of hypothalamic glioma, making it hard to distinguish from craniopharyngioma. Clinical presentation includes headache, visual disturbances, failure to thrive, hyperactivity and endocrinal disturbances such as diabetes insipidus.

On CT scans, hypothalamic gliomas are hypodense compared to the gray matter whereas on MRI, the mass (figure 4) is hypointense to isointense on T1 weighted images and hyperintensive on T2 weighted images. The contrast enhancement is variable but usually mildly homogeneous. Large gliomas may have cystic component that is hypodense on CT and hyperintense on T2 weighted MRI. T2 weighted images are useful for delineating the spread of tumor along the optic tract. Angiography is performed in case of giant and rapidly growing tumors with signs of malignant transformation identifying cerebral vessel displacement and enhancement of abnormal vascular tumor net. Treatment is based on the aggressiveness of the tumor and often involves the combination of surgery, chemotherapy and radiotherapy (23-24).

Craniopharyngioma

Craniopharyngioma (CPH) is a benign tumor, which derives from Rathke's pouch. It is postulated to arise from cells of the embryonic epithelium lining the pharyngeal-pituitary passage extending from the bottom of third ventricle up to the wall of pharynx. It constitutes 10% of all pediatric brain tumors, 90% of all pituitary masses and 56% of all chiasmal-sellar tumors. Two varieties have been identified including cystic (or adamantinomatous) tumors (ACPs) and squamous-papillary variety that are markedly different both clinically and pathologically.

ACP is more commonly seen and is often noted in pediatric patients (between 5-10 years of age). It is characterized by one or more large cysts with variable wall thickness and central proteinacious fluid that has machine oil consistency. In addition, it also has variable proportion of solid component. Overall, it is an inhomogeneous mass commonly associated with both solid and cystic component and some degree of calcification in more than 90% of cases. It is commonly seen in sellar and suprasellar location.

Squamous papillary variant is often solid in nature and rarely present with cystic component. Calcification is not commonly seen. They are often large masses and lead to mass effect and location specific manifestations. Patient often develop Horner syndrome, neurological deficit, epilepsy, headache, pseudotumor cerebri and elevation in intracranial pressure.

It is associated with CDI both before and after the curative surgery with higher incidence noted postoperatively. Interestingly, patients who underwent transfrontal removal of craniopharyngioma have no biologically active ADH in the serum despite elevated level of immunoreactive ADH. In addition, replenishment of ADH level is not effective. This presentation mimics nephrogenic DI. However, CDI in this setting is often transient.

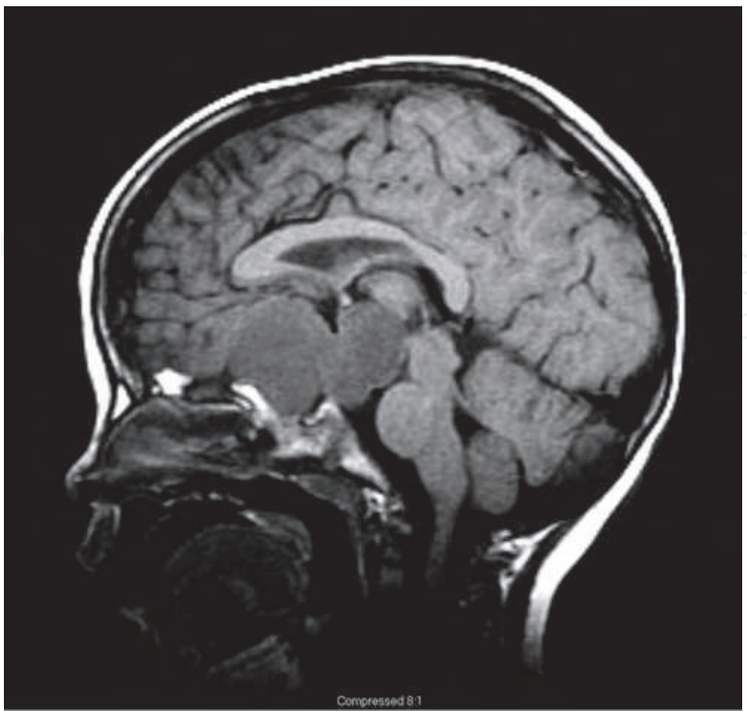

(a)

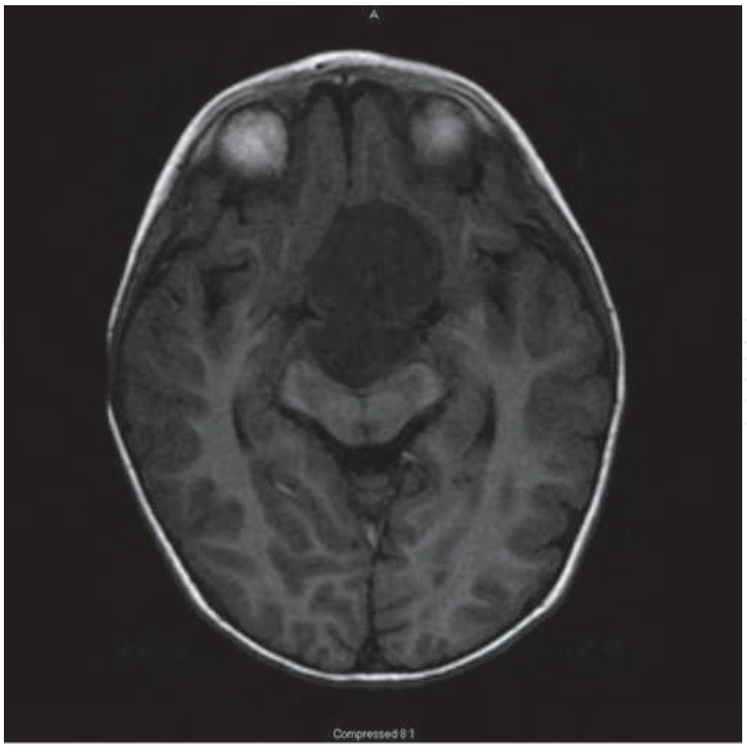

(b)

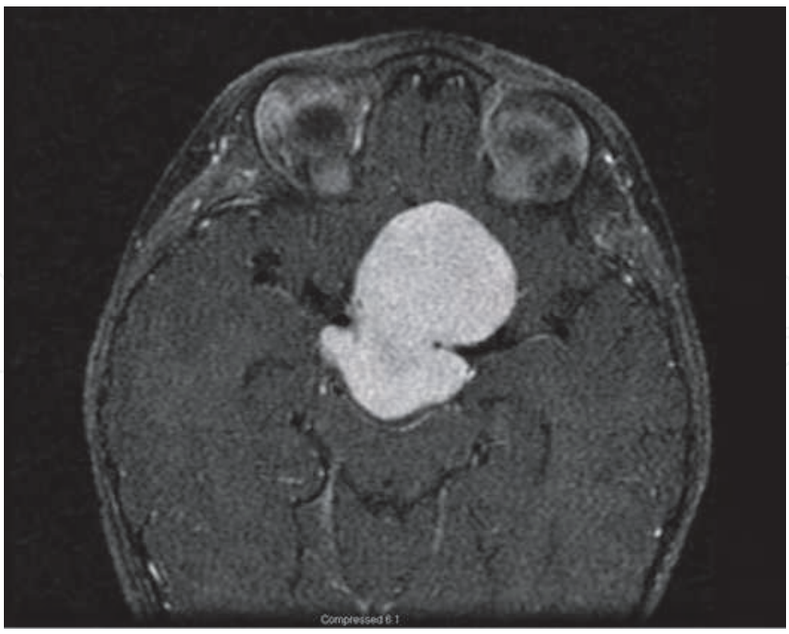

(c)

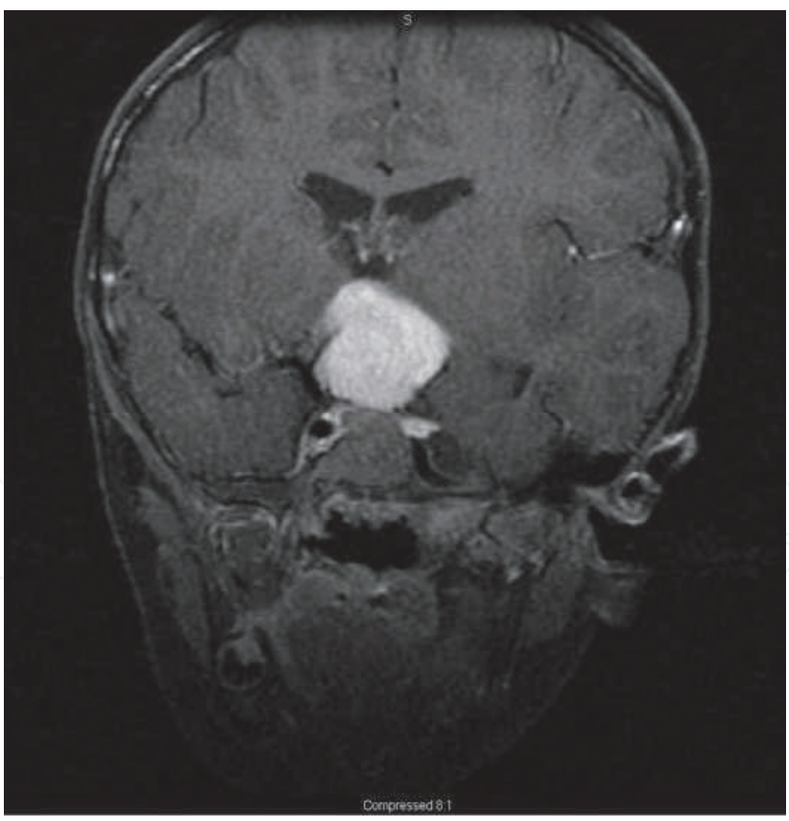

(d)

Fig. 4. Hypothalamic Glioma: Precontrast sagittal T1 (a), axial T1 (b), post contrast axial T1 (c) and coronal T1 (d) images of pilocytic astrocytoma involving hypothalamus

Imaging is very important for identifying CPH, and for delineating the location and extent of craniopharyngioma (figure 5). For example, plain radiography reveals changes in shape and size of the sella turcica, deformity of the anterior clinoid process along with calcifications in the chiasmal–sellar region. In addition, calcification is often seen within the cavity of sella and often present as laminar pattern of calcification within the capsule. In majority of the patients with CPH, the dorsum sella turcica is shortened. Mass effect on the third ventricle causes increase in intra-ventricular pressure with dilatation of ventricular system and widening of bony sutures. CT and MRI provide more detailed and accurate description of CPH, including precise size of the tumor, proportion of solid and cystic component, location, and involvement of ventricular system and erosion into adjacent structures.

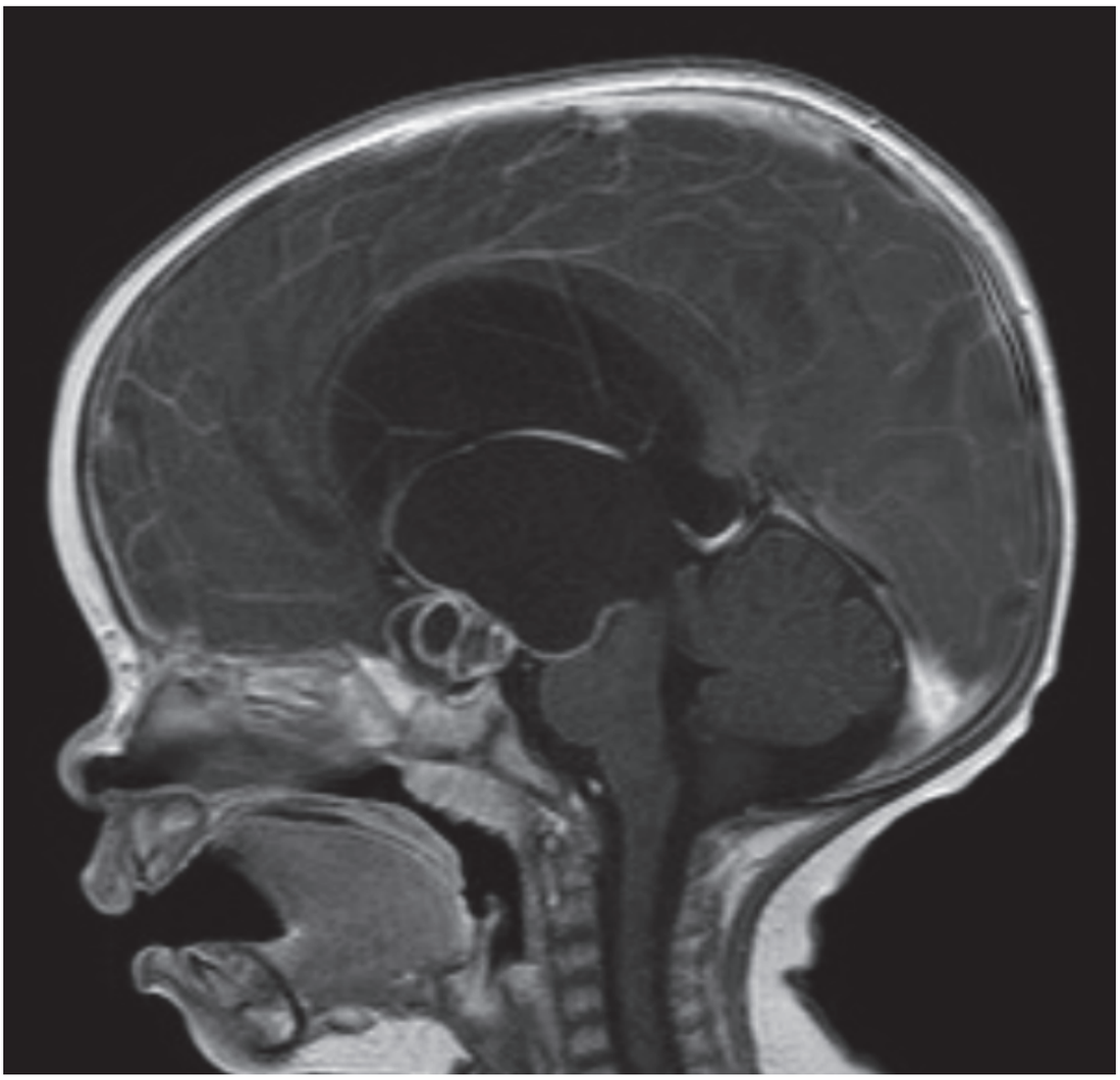

Fig. 5. Sagittal T1W post contrast MR image shows a complex solid and cystic sella-supra sellar enhancing mass. This was a proven Craniopharyngioma on histopathology.

On CT, it appears as a well defined mass with heterogeneous density. Solid part is isodense to the brain but cystic part is usually hypodense than that of brain. Density of solid component increases considerably upon contrast enhancement. CT may show hypodense lesion within the ventricles with peripheral rim of calcification. T1 weighted MR images of cystic component are often heterogeneous ranging from hypointense to hyperintense signal depending on the protein content of cyst whereas the solid or nodular part of tumor is usually isointense. On T2 weighted images, cystic area appears hyperintense with hypointense foci representing calcification. Proteinacious nature of the cystic fluid causes hyperintense signal on T1weighted images and mild hyperintensity on T2-weighted imaging at the periphery. On sagittal images, sedimentation phenomenon of cystic content can be seen. On MRI, intense contrast enhancement is seen in the wall of the cyst and also in the solid component of the tumor (25-26).

Intracranial germ cell tumors

Intracranial germ cell tumors often located close to the midline and could be both benign and malignant. Germ cell tumors arise due to defective migration of primordial germ cells and are commonly seen within the gonads, mediastinum or in the pineal region. In fact more than 50% of tumors within the pineal regional are germ cell tumors. It usually presents between the age of 10-12 years and males are more frequently affected if tumor is located within the pineal regions whereas slight female preponderance is noted in case of suprasellar germ cell tumors. Most of the intracranial germ cell tumors are within the pineal region and 20% are seen in suprasellar region and few are identified in the pituitary fossa. AFP and b-HCG levels are elevated in patients with germ cell tumor and are routinely used for screening purpose and monitoring response to treatment. They constitute 3-5% of pediatric intracranial tumors and 0.5-1% of adult intracranial tumors. Common clinical features are endocrinal disturbances such CDI, precocious puberty and panhypopituitarism. In addition, obstructive hydrocephalus, visual defects and optic nerve atrophy are also seen. On CT, germ cell tumors (figure 6) appear as hyperdense lesions with homogeneous contrast enhancement. It often shows abnormal subtle pituitary stalk thickening and enhancement in patients with CDI. On MRI, germinoma are isointense or mildly hypointense on T1 weighted images and isointense or mildly hyperintense on T2 weighted images. Strong contrast enhancement is seen on both CT and MRI. Treatment of choice is radiotherapy with excellent prognosis. Chemotherapy is used in radiotherapy resistant tumors (27-28).

Teratoma

Teratomas are usually benign tumors which contain elements derived from all the three germ layers and are covered by a capsule. They are commonly seen in pediatric male patients. When located intracranially, these lesions have predilection for the midline and involve the pineal region, the third ventricle, and the infundibulochiasmal region. Rarely, intracranial suprasellar teratomas extend into the pituitary fossa, with enlargement of the sella turcica, thereby resulting in visual disturbance, DI, and hypopituitarism.
Sella is often enlarged with widening of the entry and depression of the bottom. Often teeth like inclusions are seen with in the sella and around it. Occasionally, initial MRI may fail to identify the mass. However, upon follow up with T1- and T2-weighted MR imaging, high signal intensities representing fat components can be seen in sellar and suprasellar areas. Very often, MRI reveals teratomas as heterogeneous mass secondary to the presence of all three germ line structures which enhance following contrast administration (29-30).

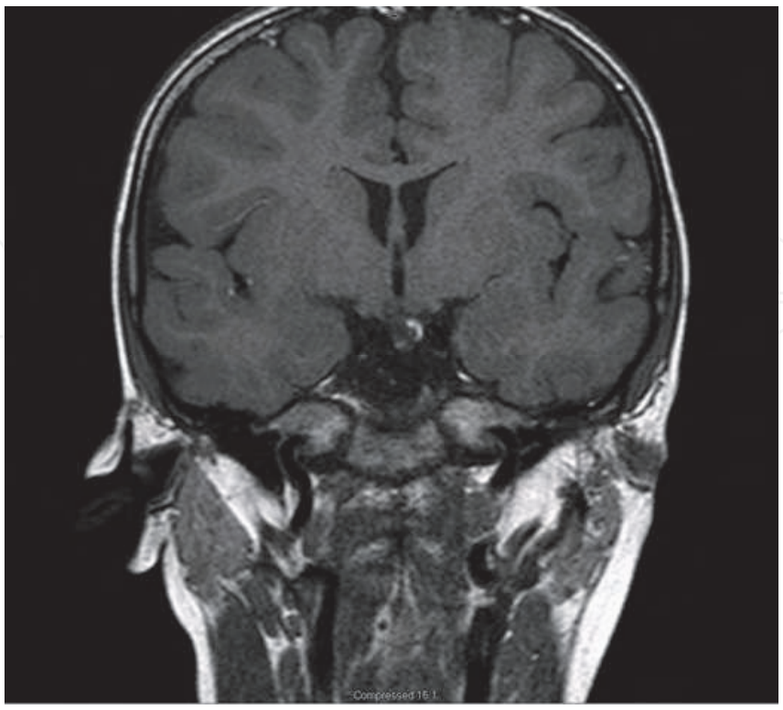

(a)

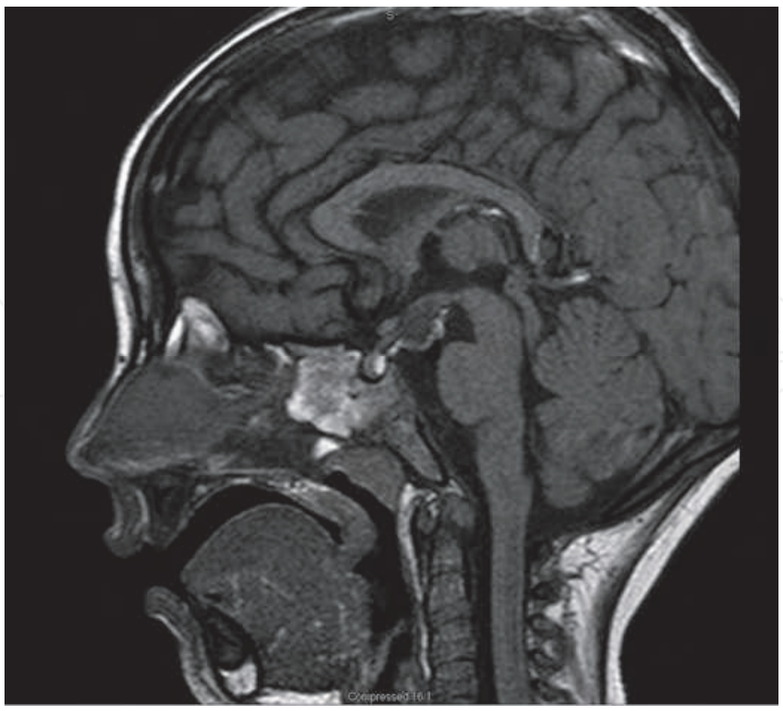

(b)

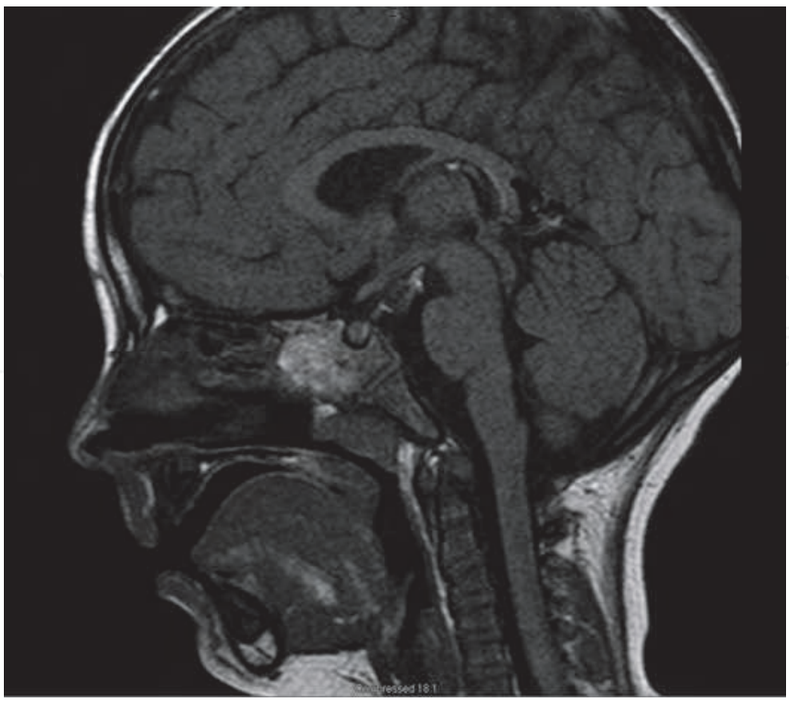

(c)

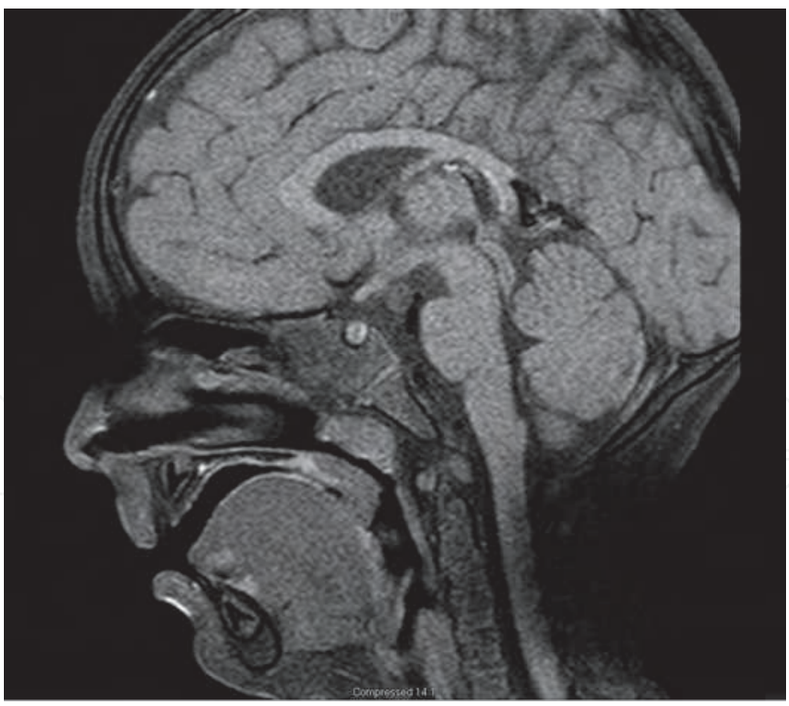

(d)

Fig. 6. Hypothalamic Dermoid: Non-fat suppressed coronal T1 (a) and sagittal T1 (b,c) shows hyperintense T1 signal in the hypothalamic mass that suppresses on fat suppressed T1 sagittal (d) image representing fat in the dermoid.

Langerhans cells histiocytosis

Langerhans Cells Histiocytosis refers to the group of granulomatous disease characterized by abnormal activation and clonal proliferation of immune cells called histiocytes or Langerhans cells and is mostly seen in children between 1-4 years of age. These cells are bone marrow derived and are a variant of dendritic cells that normally reside in the skin. Upon entry of foreign antigen into body via breach of skin, these cells engulf and process these antigens and migrate to the nearby lymph node. They present these antigens to the macrophages and other immune cells and activate the cascades of both cellular and humoral immune response against the foreign antigen. However, upon abnormal activations, these cells can lead to the granumatous disease causing erosive and painful bone lesion in addition to effect on multiple other organ systems.

There are three variants of histiocytosis including malignant (true histiocytic lymphomas), reactive (benign histiocytosis) and Langerhans cell histiocytosis (LCH). Depending upon the nature of bone involvement, LCH is further classified into three variants including unifocal, multifocal unisystem, and multifocal multisystem. In all these variants, LCH provokes nonspecific immune response and leads to painful bone swelling, erosive bone lesion and pathologic fractures, hepatosplenomegaly, lymphadenopathy, pancytopenia, infection, fever, skin rash, hormonal disturbances including diabetes insipidus, chronic cough, shortness of breath and granulomatous lung disease. LCH is commonly seen in pediatric patients and twice common in boys than girls.

Frontal bone is most commonly involved however any bone can be affected and develops punched out lesions with sharp margins and no sclerosis. Particularly, chronic recurrent form is referred as Hand-Schuller-Christian disease which presents as a triad of Diabetes insipidus, proptosis and destructive bone lesions. On the other hand, acute form of disease is called as letterer-siwe disease which presents with hepatomegaly, splenomegaly, fever, eruptive skin lesion, thrombocytopenia and anemia. Diagnosis is established via biopsy and immunohistochemistry with positive reactivity for CD1a and S-100 proteins. In addition, electron microscopy shows abnormal membranous aggregates of endoplasmic reticulum in tennis racket shaped or rod shaped structures called birbeck granules or birbeck bodies (200-400 nm in width). These bodies characteristically show central linear density and a striated appearance and are regarded as pathognomic of histiocytosis. It is reported that formation of these bodies is induced by Langerin (CD207), which is transmembrane II surface receptor present on the membrane of Langerhans cells. Clinically, several hormonal disturbances are seen but the most common is diabetes insipidus followed by growth retardation. In addition, galactorrhea, hypogonadism and hypopituitarism are also occasionally seen secondary to histiocytic infiltration of hypothalamus and partial or complete inhibition of the release of hypothalamic trophic hormones which subsequently suppresses pituitary hormonal release.

On radiographs, variable sized lytic foci are seen with characteristic beveled edge appearance of lesion margin. Occasionally, focal residual bone lesion with button sequestrum is also seen lying centrally within the area of lytic lesion. On CT scan, button sequestrum lesions are seen as sharply defined hypodense intradiploic bony defects. In addition, lytic foci and erosive changes are also seen on CT scans. On MRI, button sequestrum lesion appears as low to intermediate intensity lesion on T1 weighted images and hyperintensity lesion on T2 weighted images. In addition, contrast enhancement with fat suppression enhances the diagnostic yield and helps identify the extent of lesion, invasion of adjacent epidural space, brain parenchyma or dural venous sinuses. In addition, scintigraphy is also helpful but show variable isotope uptake, such as smaller lesions show

enhanced uptake and less or no uptake in bigger lesions. This modality help identify multiple osseous and tissue lesions and is of use for narrowing the differential diagnosis. Pituitary MRI (figure 7) will show enhancing thickened pituitary stalk (31-32).

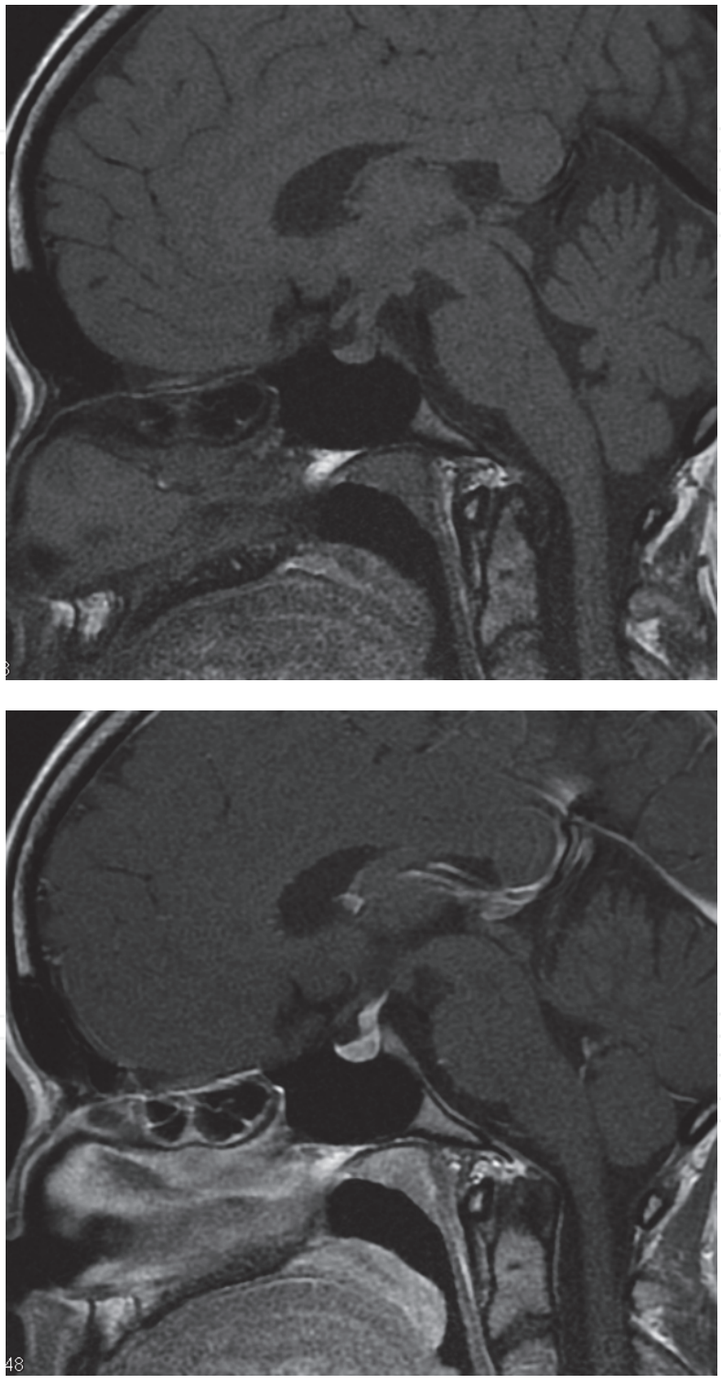

Fig. 7. Histiocytosis involving the pituitary infundibulum. Sagittal non contrast T1W MR image (top) shows absent posterior pituitary bright spot with thickened enhancing pituitary infundibulum on post contrast T1W sagittal MR image (bottom).

6.3.4.2 Adult neoplastic causes

Metastasis

Metastases to the pituitary-hypothalamic axis account for less than 1% of all the sellar masses. Breast cancer metastases are most common, accounting for 6-8% of all the metastasis to the pituitary followed by lung and GI cancers. When cancers metastasize to pituitary, most cancers involve the neurohypophysis but breast cancer demonstrates high affinity for the adenohypophysis. DI is the most common presenting symptoms in such patients and is seen in about 20% of such patients. Other manifestations include vision problems, anterior pituitary dysfunction, headache and ophthalmoplegia. It is permanent if SOP and PVN nuclei of hypothalamus are involved. If SON and PVN nuclei are spared and only posterior lobe of the pituitary is involved, than CDI is often transient.
MRI is very useful for diagnosis and shows a destructive and inhomogeneously enhancing lesion extending across intrasellar and suprasellar location. In addition, diffuse enlargement of the gland, thickening of the pituitary stalk, invasion of the cavernous sinus, and sclerosis of the surrounding sella turcica can also be noted. If metastasis is localized to the skull base, sclerosis of sella turcica is more obvious. On the other hand, if metastasis is located within the pituitary parenchyma, sella turcica sclerosis is minimal (33).

7. Psychogenic Diabetes Insipidus

It is caused by compulsive intake of large amounts of fluid leading to inhibition of normal vasopressin. Obviously, there are no imaging features of this entity. Exclusion of any intracranial lesion by MRI of brain and sella with and without contrast might aid in its diagnosis (2).

8. Nephrogenic Diabetes Insipidus (NDI)

a. **Primary**: It is X-linked recessive condition with unresponsiveness of the tubules and collecting system to vasopressin. For obvious reasons there are no specific imaging features of this entity.
b. **Secondary**: Polycystic kidney disease, drug toxicity such as Lithium toxicity, analgesic nephropathy, reflux nephropathy, amyloidosis, acute tubular nephropathy.

Polycystic kidney disease

Polycystic kidney disease (also known as PKD) is the most common life threatening genetic disorder of kidney can be either autosomal recessive (AR) or autosomal dominant (AD). Both ADPKD/ARPKD are characterized by the development of multiple cysts in both the kidneys, which are often fluid filled leading to increase in size of kidneys.
ADPKD is the most common inherited kidney disease and is postulated to have begun during the embryonic life with fewer than 5% of nephrons being affected at the time of birth. Because of fluid accumulations, cysts continue to grow and cause pressure atrophy of renal parenchyma and worsening of renal failure. Increase in serum creatinine is noted during the second and third decade of life with obvious renal failure during 6^{th}-7^{th} decade of life. Clinical features include abdominal discomfort and pain (most common), hematuria, urinary tract infection, high blood pressure, intracranial bleeding, nephrolithiasis, colon diverticulosis, hepatic cysts, pancreatic cysts, splenic cysts, cysts in seminal vesicle, cardiac cysts, arterial aneurysms (cranial vessels and aorta), abdominal wall hernias, aortic and

mitral valve abnormalities, end stage renal disease, kidney failure and occasionally nephrogenic diabetes insipidus (34-35).

Autosomal recessive PKD (ARPKD) is also called infantile PKD since signs of kidney involvement are often identified even before the birth of child. Children often die within the first few days because of respiratory difficulties arising because of lung hypoplasia secondary to oligohydramnios. In addition, with increasing age, liver scarring is also noted in children.

The diagnosis of PKD is established via imaging (figure 8). Expansile fluid filled cysts of various sizes along with distorted renal cortex and medulla in addition to stretching and elongation of kidney tubules and blood vessels are often noted. Ultrasound is recommended for the initial screening because of ease of performance, easy availability, low cost and no risk of radiation. But, the data obtained with ultrasound is often not reproducible and as accurate as compared to which is obtained via CT or MRI. Occasionally other complications also develop such as infection, hemorrhage, cyst rupture and peritonitis that can also be identified on cross sectional CT or MRI. CT is also useful for volume measurement and assessing structural defects in kidney, however, it involves the use of contrast and radiation.

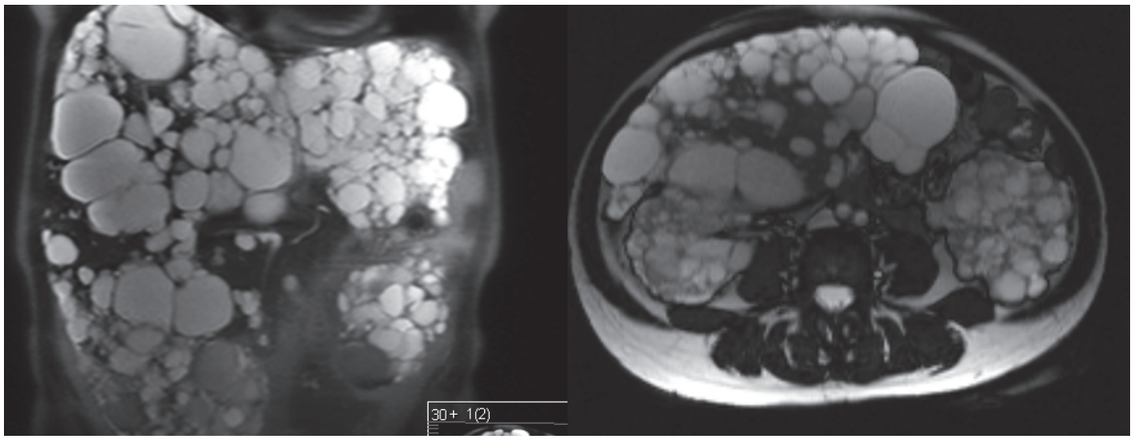

Fig. 8. Coronal HASTE (left) and axial TRUE-FISP (right) MR images show both kidneys completely replaced by cysts appearing as bright rounded structures. Notice non-visualization of any normal renal parenchyma. The patient incidentally also had Polycystic Liver Disease.

Recently, MRI has gained popularity for determining the kidney volume and estimation of disease progression. The data obtained via MRI is often reproducible and accurate in addition to excellent tissue contrast, high resolution 3D images and no need of contrast or radiation. Excellent visualization of renal cyst is obtained via coronal T2 weighted and axial fat saturated T2 weighted imaging showing hyperintense cysts throughout both kidneys. In addition, simple and complex cysts are easily differentiated with T1 weighted imaging. Contrast MRI enable better visualization of renal parenchyma however, use of gadolinium contrast can lead to development of nephrogenic systemic sclerosis in such patients with impaired kidney functions. In addition, MRI also evaluates the blood flow to the affected kidney, which is an important marker of disease progression. With increase in severity of disease, the renal blood flow decreases proportionally. In addition, imaging is also very important based on the reports that combined renal volume is a prognostic indicator of disease severity. CT and MRI are often used for volume measurement over the short period

of time whereas in patients with long interval between consecutive follow up, ultrasound is the preferred modality. In addition, other quantitative imaging markers, which are often linked with disease progression, are size, number, spatial distribution, individual growth rate, and asymmetry of cysts. MRI is very often used for measuring and evaluating these markers of disease progression. In addition, family history and genetic testing are also important in diagnosing PKD. In addition, specific anatomic areas can also be evaluated with MRI. Review of literature suggests that kidneys can weigh as much as 8 kg (normal weight is 120-140 gram) secondary to the presence of multiple fluid filled cysts (measuring up o 3 cm) and have length up to 40 cm. In one recent study, it was found that volume of kidney affected by ADPKD was up to 1000 ml (in normal people, mean volume of kidney is 150 ml). Overall, MRI is superior to ultrasonography and CT. MRI efficiently detects small renal cysts as small as 2 mm that are likely to be missed on CT and ultrasound (US). However, MRI is more expensive, less readily available, takes longer time to acquire images and is contraindicated in certain population such as those with pacemakers and other prosthesis. Some of these limitations should be overcome by technical advancements. In addition family history and genetic testing are also used for establishing the diagnosis (34-35).

Lithium nephropathy

Lithium is a well established treatment for affective disorders. It has a narrow therapeutic window, ranging from 0.6 - 1.2 mMol/L. Lithium nephrotoxicity can be classified into nephrogenic diabetes insipidus, acute toxicity, and chronic renal disease. Nephrogenic diabetes insipidus is characterized by polyuria and polydipsia. Mild toxicity can be seen at serum lithium levels of 1.5 - 2.5 mMol/L, with moderate toxicity at levels of 2.5 - 3.5 mMol/L (36).

Lithium toxicity affects multiple organ systems, and may cause coarse tremors, neuromuscular excitability, muscle weakness, sluggishness, nausea, vomiting, diarrhea, and seizures. Rhabdomyolysis can also occur. Decreasing renal function, evidenced by increasing serum creatinine and decreased creatinine clearance, is seen in chronic lithium nephropathy. The only established risk factor is lithium therapy, and an increased duration of therapy increases the risk of progression to end-stage renal disease (ESRD). Discontinuation of lithium therapy does not ensure against progression to ESRD. Chronic lithium nephropathy is a progressive condition, and pathology demonstrates tubular atrophy, glomerulosclerosis, interstitial fibrosis, and distal tubular dilatation with microcyst formation. A recent study found that tubular microcysts were present in 62.5% of renal biopsies performed in patients treated with lithium, involved both the renal cortex and medulla, and measured 1-2 mm in diameter. A serum creatinine level of 2.5 mg/dL at the time of biopsy was found to be the only significant predictor of progression to ESRD (36).

Renal cystic disease is commonly evaluated with US, computed tomography (CT), and MRI. US demonstrates well-circumscribed, anechoic cystic structures with posterior acoustic enhancement, and CT shows hypodense cystic structures measuring between -10 and +20 Houndsfield units (HU). The number and nature of cystic lesions is best characterized by MRI, and T2-weighted imaging most accurately assesses the fluid content of lesions. MRI is a useful tool to evaluate the renal parenchyma, and when combined with magnetic resonance angiography (MRA), can effectively study the renal arteries. T2-weighted images demonstrate the microcysts of chronic lithium nephropathy as small hyperintense 1-2 mm

round lesions. In a patient with a history of lithium therapy, MR imaging of abundant microcysts within the kidneys bilaterally strongly supports the diagnosis of chronic lithium nephropathy, and may obviate the need for renal biopsy (36).

Analgesic nephropathy

Analgesic nephropathy is defined as damage to one or both kidneys resulting from chronic exposure to over the counter pain medications such as acetaminophen and NSAIDs or other medications containing phenacetin. It has been suggested that approximately 6 or more pills for 3 years significantly increases the risk for analgesic nephropathy. It is seen in 4 per 100,000 thousand patients and is more common in female above 30 years of age, most of whom are self medicating for relief from chronic pain. It is more common in Europe, Australia and USA. However, its incidence has declined significant in the past few decades owing to decreased consumption of phenacetin containing compounds and public awareness (43-44).

Initial changes include scarring of small blood vessels called capillary sclerosis which in turn lead to renal papillary necrosis and subsequently chronic interstitial nephritis. In the absence of treatment and avoidance of analgesics, patient develops pyelonephritis, renal failure, anemia, high blood pressure, NDI and end stage renal disease. These changes are postulated to result from decrease blood flow to the kidney because of vessel sclerosis and also because of inhibition of prostaglandin E2 production by NSAIDs, depletion of antioxidants and oxidative damage to the kidney.

Both CT and US can be used for assessing kidney damage because of analgesic nephropathy and show bilateral decrease in renal volume combined with either bumpy contours or papillary calcifications. However, US has higher sensitivity than CT scan for detecting RPN due to analgesic nephropathy (37-38).

Reflux nephropathy

Reflux nephropathy (RN) caused because of reflux of urine back into kidneys instead of going forward into the bladder and then into urethra. It is caused because of defective valve at the site of insertion of ureter into bladder and the condition is vesico-ureteric reflux (VUR). Over the period of time, reflux of urine back into kidneys injures the parenchyma and causes small and scarred kidneys. Scarring is almost always seen and often develops within the first five years of life. In addition, patient also develops hypertension, hematuria, proteinuria, chronic renal failure, ESRD and NDI. Recurrent urinary tract infection in male and female children raises the suspicion for RN and warrant further investigations. Initial investigations of choice are ultrasonogram, voiding cystourethrography and renal scientigraphy or nuclear cystography using Tc 99m dimercaptosuccinic acid (DMSA). DMSA scan is now regarded as the most sensitive and specific modality for detecting inflammatory changes within the kidney and also for identifying VUR, particulary the transient episodes and uses low radiation dose. In recent study it was found that DMSA scan was positive in children with negative vesicocysto urethrogram (VCUG), indicating higher sensitivity with DMSA scan. Chronic reflux nephropathy in adult can also be evaluated with IV excretory urography or nephropyelotomography or CT urography, which often reveals calyceal distortion with typical claviform morphology. In addition, dilatation of intra-renal urinary tract is also seen. On voiding cystourethrogram, backward flow of contrast from opacified bladder into the ureter is seen in patients with VUR. In addition, contrast enhanced CT or MRI can also show parenchymal changes such as decrease in renal

size and presence of notch of the renal parenchyma surface, parencymal scarring, ureteral dilatation and calyceal clubbing. Long standing reduction in renal mass often leads to glomerular injury and sclerosis. Contrast-enhanced voiding sonocystography is a newer modality and useful alternative. This modality is radiation free and uses microbubble-based contrast agents. Recently, it has been proposed that contrast-enhanced voiding sonocystographyshould be used for both diagnosis and follow up of patients with VUR since several recent studies have shown superiority of Contrast-enhanced voiding sonocystography over VCUG and nuclear cystography for detecting VUR. In addition, MR urography (MRU) is an excellent modality and provides detailed information regarding the anatomy (such as renal contour and caliceal configuration) and functioning of urinary tract. It is suggested that in many ways MRU is more useful than DMSA scan. Recently, Lonergan et al. demonstrated that gadolinium-enhanced inversion-recovery MR imaging has higher sensitivity for detecting focus of infections within the urinary tract and offer greater reproducibility. In addition, MRU provides greater resolution, excellent tissue contrast, detailed analysis of tubular function without causing background artifact and radiation exposure. However, it is an expensive and time consuming modality and requires sedation, which negates its usefulness to some extent (39-41).

Amyloidosis

Amyloidosis is a group of heritable or acquired diseases characterized by the deposition of abnormal proteinacious material as beta-fibrillar sheets in the extracellular space. It can affect almost every organ system either alone or in combination. Primary amyloidosis develop secondary to immune disorder such as multiple myeloma where as secondary amyloidosis is often due to chronic inflammatory diseases such as rheumatoid arthritis. Definitive diagnosis is established with biopsy followed by tissue staining with special dyes. The commonly used staining agent is Congo Red Dye which causes apple green bifringence under polarized light and thioflavine-T (intense yellow-green fluorescence). In addition, imaging can also be crucial for managing patients affected with amyloidosis. Its utility however has been limited due to the fact that imaging findings are often nonspecific and diverse (42-43).

Renal involvement in multiple myeloma (MM) and rheumatoid arthritis (RA) leads to small and contracted kidneys. CT may show either focal cortical mass with focal calcifications or diffuse infiltration in the kidney glomeruli or interstitium. Variability in kidney size reflect the stage of disease. For example, during the acute stage, kidneys may be enlarged with smooth contour whereas in chronic phase kidneys are often shrunken with diffuse irregular contour, thinned cortex and hard texture (called as amyloid contracted kidneys). In addition, diffuse cortical thinning is also noted in chronic phase in addition to focal parenchymal nodules. Other findings noted in renal amyloidosis are amorphous calcification of renal parenchyma, filling defect in renal pelvis either because of blood clot or because of amyloid mass and perinephric mass with calcification. In addition, decreased renal perfusion and reduced elimination of contrast can also be seen on urography and/or angiography in these patients.

On ultrasound, renal amyloidosis often meets the criteria for type 1 renal parenchymal disease. Increase in echogenecity of renal cortex is noted along with medullary prominence which is suggested to be due to the deposition of amyloid, calcium or acute parenchymal diseases. In addition, corticomedullary demarcation is often prominent and arcuate vessels are obscured (42-43).

Recently, it has been suggested that diffusion weighted MRI is also of use in evaluating renal amyloidosis in patient with familial Mediterranean fever. In addition, nuclear scan performed after administration of gallium show enhanced uptake in affected kidneys and is suggestive of disease activity. However, PET/CT failed to show enhanced uptake in case of cardiac and renal amyloidosis (42-44).

Acute tubular necrosis

Acute tubular necrosis or (ATN) is characterized by the death of tubular cells in kidney. Tubular cells constitute kidney tubules, which are key structures for transferring urine to the ureter. These cells also perform reabsorbtion of 99% of water filtered into Bowman's capsule and concentrate the urine. Tubular cells possess regenerating capacity and continuously replace the old and dying cells. This is very important and allows for complete recovery from ATN if precipitating cause is eliminated. ATN often presents with ARF and is the most common cause of ARF. There are two varieties of ATN. One is ischemic ATN and another one in toxic ATN. Ischemic ATN occurs due to decreased perfusion (renal artery stenosis, shock, renal artery emboli) whereas toxic ATN occurs due to exposure to toxins (such as analgesics or antibiotics, hemoglobin, myoglobin, Bence Jones proteins of multiple myeloma, heavy metals, organic solvents, posion and several others). Since the damage occurs to the kidney, it is classified as renal cause of acute renal failure. Urinalysis often shows pathognomonic muddy brown epithelial cast in patients with ATN along with increased fractional excretion of sodium (>3%). Histopathology shows tubulorrhexis, which is a localized necrosis of the epithelial cells lining the renal tubules. In addition, focal rupture or loss of basement membrane is also seen developing skip lesions through the tubules. Due to loss of basement membrane, regeneration is often unlikely in ischemic ATN. In toxic ATN, basement membrane is often intact and allows complete recovery if precipitating cause is removed in timely manner. However, in both types, dead or partially viable cells shed into tubular lumen and lead to obstruction and eventual renal failure. Ultrasound and renal scintigraphy are useful for evaluation and diagnosis of ATN. US show swollen and enlarged pyramids with decreased cortico-medullary differentiation and increased resistive index. On the other hand renal scintigraphy shows normal perfusion, increased retention and decreased excretion (45-46).

9. References

[1] Maghnie M. Diabetes insipidus. Horm Res. 2003;59 Suppl 1:42-54. Review.
[2] Dundas B, Harris M, Narasimhan M. Psychogenic polydipsia review: etiology, differential, and treatment. Curr Psychiatry Rep. 2007 Jun;9(3):236-41.
[3] Maghnie M, Cosi G, Genovese E, Manca-Bitti ML, Cohen A, Zecca S, Tinelli C, Gallucci M, Bernasconi S, Boscherini B, Severi F, Aricò M. Central diabetes insipidus in children and young adults. N Engl J Med. 2000 Oct 5;343(14):998-1007.
[4] Morello JP, Bichet DG. Nephrogenic diabetes insipidus. Annu Rev Physiol.2001;63:607-30.
[5] Bichet DG. Nephrogenic diabetes insipidus. Adv Chronic Kidney Dis. 2006 Apr;13(2):96-104.
[6] Mazumdar A. Imaging of the pituitary and sella turcica. Expert Rev Anticancer Ther. 2006 Sep;6 Suppl 9:S15-22.

[7] Elster AD. Imaging of the sella: anatomy and pathology. Semin Ultrasound CT MR. 1993 Jun;14(3):182-94.
[8] Zee CS, Go JL, Kim PE, Mitchell D, Ahmadi J. Imaging of the pituitary and parasellar region. Neurosurg Clin N Am. 2003 Jan;14(1):55-80, vi.
[9] Arima H, Oiso Y. Mechanisms underlying progressive polyuria in familial neurohypophysial diabetes insipidus. J Neuroendocrinol. 2010 Jul;22(7):754-7.
[10] Carman KB, Yarar C, Yakut A, Adapinar B. Septo-optic dysplasia plus: a patient with diabetes insipidus. Pediatr Neurol. 2010 Jul;43(1):76-8.
[11] McCabe MJ, Alatzoglou KS, Dattani MT. Septo-optic dysplasia and other midline defects: the role of transcription factors: HESX1 and beyond. Best Pract Res Clin Endocrinol Metab. 2011 Feb;25(1):115-24.
[12] Guillemin R. Neuroendocrinology: a short historical review. Ann N Y Acad Sci. 2011 Mar;1220:1-5. doi: 10.1111/j.1749-6632.2010.05936.x.
[13] Sharma RR. Hamartoma of the hypothalamus and tuber cinereum: a brief review of the literature. J Postgrad Med. 1987 Jan;33(1):1-13. Review.
[14] Boyko OB, Curnes JT, Oakes WJ, Burger PC. Hamartomas of the tuber cinereum: CT, MR, and pathologic findings. AJNR Am J Neuroradiol. 1991 Mar-Apr;12(2):309-14.
[15] Levitt MA, Fleischer AS, Meislin HW. Acute post-traumatic diabetes insipidus: treatment with continuous intravenous vasopressin. J Trauma. 1984 Jun;24(6):532-5.
[16] HAY DR. Diabetes insipidus after tuberculous meningitis. Br Med J. 1960 Mar 5;1(5174):707.
[17] Tabuena RP, Nagai S, Handa T, Shigematsu M, Hamada K, Ito I, Izumi T, Mishima M, Sharma OP. Diabetes insipidus from neurosarcoidosis: long-term follow-up for more than eight years. Intern Med. 2004 Oct;43(10):960-6.
[18] Bihan H, Christozova V, Dumas JL, Jomaa R, Valeyre D, Tazi A, Reach G, Krivitzky A, Cohen R. Sarcoidosis: clinical, hormonal, and magnetic resonance imaging (MRI) manifestations of hypothalamic-pituitary disease in 9 patients and review of the literature. Medicine (Baltimore). 2007 Sep;86(5):259-68.
[19] Cunnington JR, Jois R, Zammit I, Scott D, Isaacs J. Diabetes insipidus as a complication of Wegener's granulomatosis and its treatment with biologic agents. Int J Rheumatol. 2009;2009:346136.
[20] Xue J, Wang H, Wu H, Jin Q. Wegener's granulomatosis complicated by central diabetes insipidus and peripheral neutrophy with normal pituitary in a patient. Rheumatol Int. 2009 Aug;29(10):1213-7.
[21] Rivera JA. Lymphocytic hypophysitis: disease spectrum and approach to diagnosis and therapy. Pituitary. 2006;9(1):35-45. Review.
[22] Cemeroglu AP, Blaivas M, Muraszko KM, Robertson PL, Vázquez DM. Lymphocytic hypophysitis presenting with diabetes insipidus in a 14-year-old girl: case report and review of the literature. Eur J Pediatr. 1997 Sep;156(9):684-8.
[23] Dziurzynski K, Delashaw JB, Gultekin SH, Yedinak CG, Fleseriu M. Diabetes insipidus, panhypopituitarism, and severe mental status deterioration in a patient with chordoid glioma: case report and literature review. Endocr Pract. 2009 Apr;15(3):240-5.
[24] Alshail E, Rutka JT, Becker LE, Hoffman HJ. Optic chiasmatic-hypothalamic glioma. Brain Pathol. 1997 Apr;7(2):799-806.

[25] Ghirardello S, Hopper N, Albanese A, Maghnie M. Diabetes insipidus in craniopharyngioma: postoperative management of water and electrolyte disorders. J Pediatr Endocrinol Metab. 2006 Apr;19 Suppl 1:413-21.
[26] Haraguchi K, Morimoto S, Tanooka A, Inoue M, Yoshida Y. [Craniopharyngioma presenting a symptom of pituitary apoplexy and hyponatremia: a case report]. No Shinkei Geka. 2000 Dec;28(12):1111-5.
[27] Tao Y, Lian D, Hui-Juan Z, Hui P, Zi-Meng J. Value of brain magnetic resonance imaging and tumor markers in the diagnosis and treatment of intracranial germinoma in children. Zhongguo Yi Xue Ke Xue Yuan Xue Bao. 2011 Apr;33(2):111-5.
[28] Kreutz J, Rausin L, Weerts E, Tebache M, Born J, Hoyoux C. Intracranial germ cell tumor. JBR-BTR. 2010 Jul-Aug;93(4):196-7.
[29] Kim YS, Kang SG, Kim YO. Pituitary teratoma presenting as central diabetes insipidus with a normal MRI finding. Yonsei Med J. 2010 Mar 1;51(2):293-4.
[30] Sandow BA, Dory CE, Aguiar MA, Abuhamad AZ. Best cases from the AFIP: congenital intracranial teratoma. Radiographics. 2004 Jul-Aug;24(4):1165-70.
[31] Carpinteri R, Patelli I, Casanueva FF, Giustina A. Pituitary tumours: inflammatory and granulomatous expansive lesions of the pituitary. Best Pract Res Clin Endocrinol Metab. 2009 Oct;23(5):639-50.
[32] Rosenzweig KE, Arceci RJ, Tarbell NJ. Diabetes insipidus secondary to Langerhans' cell histiocytosis: is radiation therapy indicated? Med Pediatr Oncol. 1997 Jul;29(1):36-40.
[33] Hermet M, Delévaux I, Trouillier S, André M, Chazal J, Aumaître O. [Pituitary metastasis presenting as diabetes insipidus: a report of four cases and literature review]. Rev Med Interne. 2009 May;30(5):425-9.
[34] Martinez JR, Grantham JJ. Polycystic kidney disease: etiology, pathogenesis, and treatment. Dis Mon. 1995 Nov;41(11):693-765.
[35] Onuigbo MA, Skalski J. Newly symptomatic central diabetes insipidus in ESRD with adult polycystic kidney disease following intracranial hemorrhage: the first reported case. Med Sci Monit. 2010 Feb 26;16(3):CS29-32.
[36] Grünfeld JP, Rossier BC. Lithium nephrotoxicity revisited. Nat Rev Nephrol. 2009 May;5(5):270-6.
[37] Jung DC, Kim SH, Jung SI, Hwang SI, Kim SH. Renal papillary necrosis: review and comparison of findings at multi-detector row CT and intravenous urography. Radiographics. 2006 Nov-Dec;26(6):1827-36.
[38] Köhler H, Weber M, Wandel E, Schild HH. [The analgesic-damaged kidney. Importance of the imaging procedure]. Dtsch Med Wochenschr. 1987 Aug 28;112(35):1347-52.
[39] Smith EA. Pyelonephritis, renal scarring, and reflux nephropathy: a pediatric urologist's perspective. Pediatr Radiol. 2008 Jan;38 Suppl 1:S76-82.
[40] Eggli DF, Tulchinsky M. Scintigraphic evaluation of pediatric urinary tract infection. Semin Nucl Med. 1993 Jul;23(3):199-218.
[41] Chang SL, Caruso TJ, Shortliffe LD. Magnetic resonance imaging detected renal volume reduction in refluxing and nonrefluxing kidneys. J Urol. 2007 Dec;178(6):2550-4.
[42] Lee VW, Skinner M, Cohen AS, Ngai S, Peng TT. Renal amyloidosis. Evaluation by gallium imaging. Clin Nucl Med. 1986 Sep;11(9):642-6.

[43] Hachulla E, Maulin L, Deveaux M, Facon T, Blétry O, Vanhille P, Wechsler B, Godeau P, Levesque H, Hatron PY, Huglo D, Devulder B, Marchandise X. Prospective and serial study of primary amyloidosis with serum amyloid P component scintigraphy: from diagnosis to prognosis. Am J Med. 1996 Jul;101(1):77-87.

[44] Kim SH, Han JK, Lee KH, Won HJ, Kim KW, Kim JS, Park CH, Choi BI. Abdominal amyloidosis: spectrum of radiological findings. Clin Radiol. 2003 Aug;58(8):610-20.

[45] Dupas B, Buzelin MF, Karam G, Vasse N, Meflah K, Bach-Gansmo T. Contrast-enhanced MR imaging of experimental acute tubular necrosis. Acta Radiol. 2001 Jan;42(1):74-9.

[46] Platt JF, Rubin JM, Ellis JH. Acute renal failure: possible role of duplex Doppler US in distinction between acute prerenal failure and acute tubular necrosis. Radiology. 1991 May;179(2):419-23.

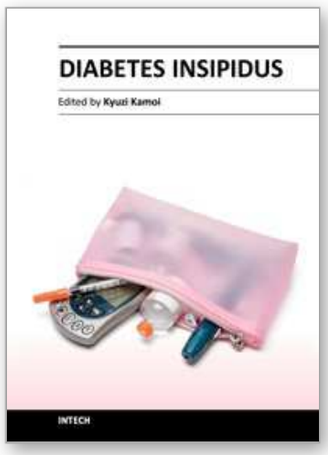

Diabetes Insipidus

Edited by Prof. Kyuzi Kamoi

ISBN 978-953-307-367-5
Hard cover, 140 pages
Publisher InTech
Published online 14, November, 2011
Published in print edition November, 2011

The first chapter of the book reports on the management of Langerhans cell histiocytosis (LCH)-induced central diabetes insipidus and its associated endocrinological/neurological sequelae in the national survey. The next chapter addresses DI and head injuries. Next, the management of neuroendocrine instability during maintenance of potential organ donors is described. Organ transplants have gradually increased worldwide. To have maintenance of appropriate potential organs, AVP is needed. Furthermore, nephrogenic DI-the potential therapeutic drugs and analysis of membrane protein stability is the topic of the next two chapters, followed by new insights into the diagnosis and management of pregnancy-related DI. The seventh chapter reports on the problems with differential diagnosis in a case of central DI in a female patient with bipolar disorder. The lithium treatment usually resulted in nephrogenic DI. Finally, over the last years, the development of MRI imaging on the pituitary gland with the stalk and hypothalamus has advanced. The final chapter interprets imaging techniques in DI in detail.

INTECH
open science | open minds

InTech Europe
University Campus STeP Ri
Slavka Krautzeka 83/A
51000 Rijeka, Croatia
Phone: +385 (51) 770 447
Fax: +385 (51) 686 166
www.intechopen.com

InTech China
Unit 405, Office Block, Hotel Equatorial Shanghai
No.65, Yan An Road (West), Shanghai, 200040, China
中国上海市延安西路65号上海国际贵都大饭店办公楼405单元
Phone: +86-21-62489820
Fax: +86-21-62489821

IntechOpen